ISSN 1980-9743

Soils and Rocks

Soils and Rocks

An International Journal of Geotechnical and Geoenvironmental Engineering

Volume 34, N. 1
January-April 2011

Soils and Rocks
Volume 34, N.1
2011

ISSN 1980-9743

SOILS and ROCKS

An International Journal of Geotechnical and Geoenvironmental Engineering

Publication of

ABMS - Brazilian Association for Soil Mechanics and Geotechnical Engineering

SPG - Portuguese Geotechnical Society

Volume 34, N. 1, January-April 2011

Table of Contents

Effects of the Construction Method on Pile Performance: Evaluation by Instrumentation. Part 2: Experimental Site at the Faculty of Engineering of the University of Porto

Paulo José Rocha de Albuquerque, Faiçal Massad, Antonio Viana da Fonseca, David de Carvalho, Jaime Santos, Elisabete Costa Esteves

Abstract. Three different types of piles (bored, CFA and precast driven) were installed in the experimental site located in the Campus of the Faculty of Engineering of the University of Porto to study the effects of the construction method on pile performance. The subsoil is a residual granitic soil reaching depth levels over 20 m. In this site, several field and laboratory tests were conducted to obtain the local geotechnical parameters. Static pile load tests with load-unload cycles were performed. Bored and CFA piles were instrumented along the depth, with installation of retrievable sensors; a flat-jack load cell was inserted at the bottom of the bored pile. Load tests results demonstrated that bored and CFA piles show similar behavior: i) the applied load reaching the pile tip was about 42%, ii) and the average mobilized lateral resistance was about 60 kPa. After the tests were completed, piles were extracted for further inspection of shaft and load cell conditions. The driven pile although having a smaller cross-section showed a stiffer response and higher resistance than the other two piles, which are a clear indication that the installation effects play an important role in the pile response. The results are compared to those obtained in Part 1 of this article relating to tests performed at the Experimental Field of Unicamp (State University of Campinas).

Keywords: construction technique, bored pile, CFA pile, precast pile, instrumentation, granitic residual soil.

1. Introduction

The use of deep foundations in the City of Porto, in the North of Portugal, has been very frequent, mainly due to the particular geotechnical conditions of that area and the great development of means and processes of construction for this type of ground conditions. Therefore, knowledge of operation and calculation parameters used in design is essential. Many factors influence the behavior of deep foundations, some of which are difficult or even impossible to be characterized, so that the design methods for piles, especially in residual soils, still remain undefined. Thus, it became important to conduct axial compressive load tests on three different piles: bored with temporary casing, CFA and precast square. Piles were executed under the same current practice conditions and utilizing internal instrumentation at depth, allowing the assessment of load distribution along the shaft. Tests were conducted at the Experimental site of the Faculty of Engineering of the University of Porto, where a broad geotechnical site investigation was carried out, including a significant number of *in situ* and laboratory tests. The experimental site is composed of granitic subsoil, characterized by a very heterogeneous residual soil (saprolitic).

This study was conducted within a project supported by specialized companies and integrated in an International Prediction Event (Class A). The event was organized by the Faculty of Engineering of the University of Porto (FEUP) and the High Technical Institute of the Technical University of Lisbon (IST-UTL) in collaboration with the TC18 of the ISSMGE and the organizers of the ISC'2 Conference in Porto in September 2004 (Viana da Fonseca & Santos, 2008).

2. Experimental Site of Feup

2.1. Geological-geotechnical characteristics

In the northern region of Portugal, granitic residual soils prevail, reaching depths over 20 m. These soils have particular characteristics as a consequence of the variability and heterogeneity in macroscopic level and, on the other hand, by the inter-particles spatial arrangement and distribution. In Portugal, a country that has temperate weather, residual soils are generally found in the northern coast, characterized by a high rainfall rate with moderate temperatures and low gradients (Costa Esteves, 2005).

Paulo José Rocha de Albuquerque, D.Sc, Faculdade de Engenharia Civil, Arquitetura e Urbanismo, Universidade Estadual de Campinas, Av. Albert Einstein 951, 13083-852 Campinas, SP, Brazil. e-mail: pjra@fec.unicamp.br.
Faiçal Massad, D.Sc., Escola Politécnica, Universidade de São Paulo, Av. Professor Almeida Prado 271, Trav. 2, Cidade Universitária, 05508-900 São Paulo, SP, Brazil. e-mail: faical.massad@poli.usp.br.
Antonio Viana da Fonseca, D.Sc., Faculdade de Engenharia, Universidade do Porto, Rua Dr. Roberto Frias 4200-465, Porto, Portugal. e-mail: viana@fe.up.pt.
David de Carvalho, D.Sc, Faculdade de Engenharia Agrícola, Universidade Estadual de Campinas, Av. Marechal Rondon 501, 13083-875 Campinas, SP, Brazil. e-mail: david@feagri.unicamp.br.
Jaime Santos, D.Sc., Instituto Superior Técnico, Universidade Técnica de Lisboa, Av. Rovisco Pai 1049-001, Lisbon, Portugal. e-mail: jaime@civil.ist.utl.pt.
Elisabete Costa Esteves, M.Sc., Instituto Superiorde Engenharia do Porto, Rua Dr. Antonio Bernardino de Almeida 431, 4200-072 Porto, Portugal. e-mail: efm@isep.ipp.pt.
Submitted on February 4, 2010; Final Acceptance on September 20, 2010; Discussion open until August 31, 2011.

The experimental site is located in the University Campus at the Faculty of Engineering of the University of Porto, Portugal. Its location is shown in Figs. 1 and 2, where the geological map of the Porto Region and the Experimental site is also shown.

It can be noticed that the site is located in a region where igneous rocks predominate: medium or medium to fine grained granite named Porto's granite. Subsoil is constituted by medium to fine particle sand (young residual soil) up to 1.5 m to 2 m thick, followed by a layer of approximately 13 m of residual soil composed of medium to fine sand (structured residual soil). Between 15 and 20.5 m, a medium particle and very weathered granite is found. Ground water table can be found at 8.5 m to 11.5 m, depending on the period of the year. Several in situ tests were conducted (SPT, CPTU, DMT, PMT and seismic tests) to characterize the soil. Laboratory tests were performed on undisturbed samples obtained from the studied site: triaxial, resonant column and oedometric tests, besides usual identification tests. The localization of these tests is represented together with the tested piles in Fig. 3. Figures 4, 5 and 6 show the variation of N_{SPT}, q_c and f_s with depth, respectively.

2.2. Execution of piles characteristics

In this experimental site, a total of 14 piles were executed; 10 were 600 mm diameter bored piles, installed using a temporary steel casing, two of which were shorter, 6 m long (E0 and E9) and eight were 22 m long. These were used as reaction piles (E1 to E8); two 600 mm diameter

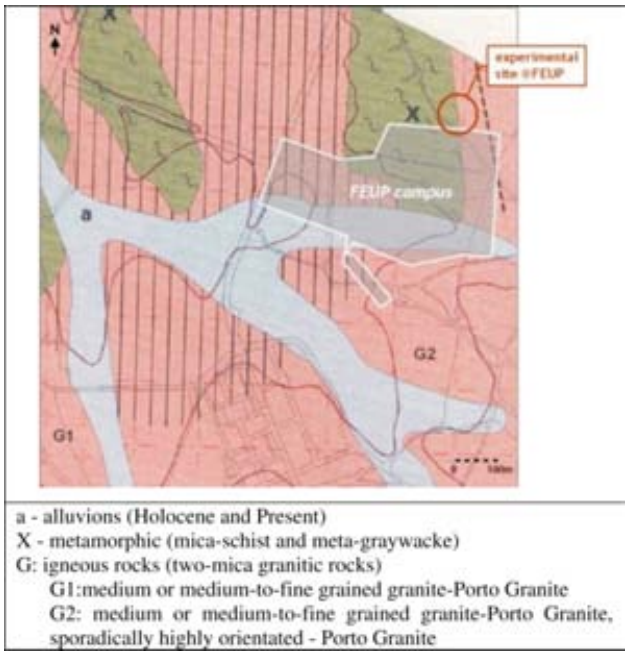

Figure 2 - Geological map of the experimental site (Viana da Fonseca *et al.*, 2004).

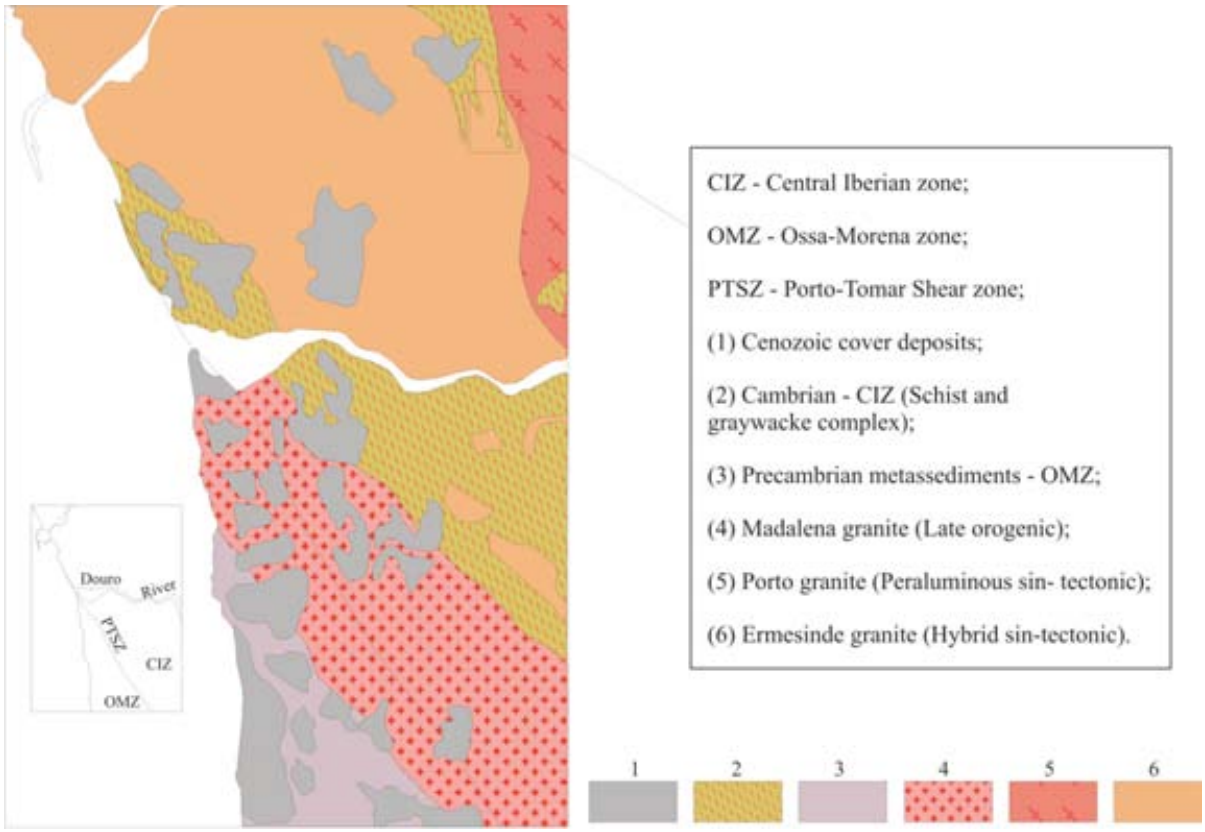

Figure 1 - Geological map of Porto Region (Viana da Fonseca *et al.*, 2004).

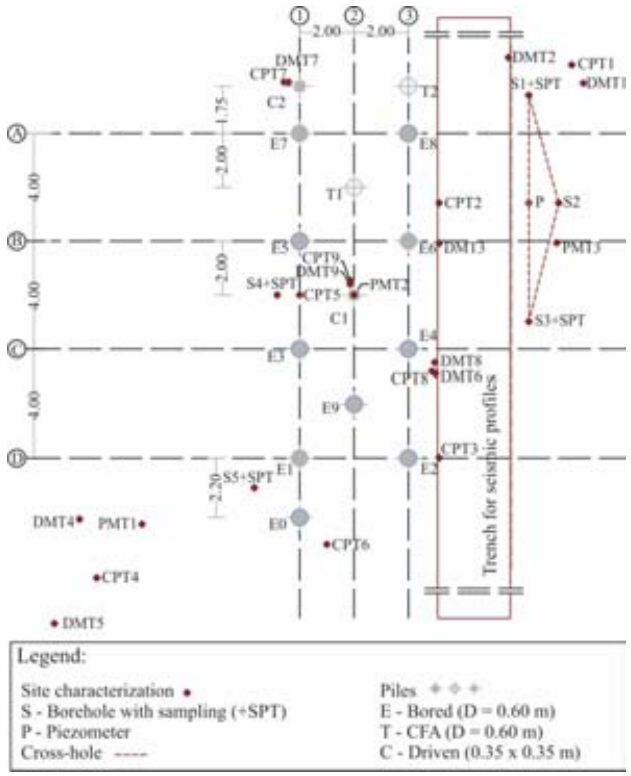

Figure 3 - Layout of the experimental site (Viana da Fonseca *et al.*, 2004).

CFA piles were installed to 6 m depth (T1 and T2) and two 350 mm square precast (C1 and C2) were precast to a depth of 6 m. Piles followed a predefined alignment and spacing between piles axis was variable but not lower than the usual recommended spacing (around three diameters).

In the static load tests, the reaction system was materialized by the eight bored and longer piles already mentioned and shown in Fig. 3 (E1 to E8 with 22 m embedded length in the soil). The test piles E9, C1 and T1 were executed with 6 m of embedded length in the saprolitic soil. Characteristics of the piles are summed up in Table 1. Details of installation of each type of pile are given in items 2.4, 2.5 and 2.6.

2.3. Load tests results

The test procedures tried to meet ISSMGE-ERTC3 (De Cock *et al.*, 2003), ASTM D 1143/94 and NBR 12.131/92 recommendations. The piles were loaded in increments with unloading cycles and for each loading stage the load was maintained until the displacement rate became less than 0.3 mm/h, with a minimum of 0.5 h and a maximum of 2 h. Maximum loads established for each pile are shown in Table 2 and load-settlement curves in Fig. 7.

2.4. Case 1 – Bored pile with temporary casing

2.4.1. Execution technique

Bored piles installed with a temporary casing are those which cause reduced soil displacement, thus, stress

Table 1 - Pile characteristics (Costa Esteves, 2005).

Piles (*)	Name	Type	Cross-section (mm)	L(m)	Longitudinal reinforcement	Transverse reinforcement	f_{ck} (***) (MPa)	f_{cm} (***) (MPa)
Reaction (tension)	E1 to E8	bored	Circular (ϕ 600)	< 12	A500 12ϕ25	ϕ12 with a 10 cm spacing	27.7	30.9
				12 < L < 22	A500 6ϕ25	ϕ12 with a 20 cm spacing		
Static (compression)	E9	Bored	Circular (ϕ 600)	6	A500 12ϕ25	ϕ12 with a 10 cm spacing	27.7	30.9
Static and dynamic (compression)	C1, C2	precast	Square (350x350)	6	A400 8ϕ16	A235 ϕ6 with a 16 cm spacing(**)	45	48
Static and dynamic (compression)	T1, T2	CFA	Circular (ϕ 600)	6	A500 12ϕ25	ϕ10 with a 10 cm spacing	44	52.6

(*)behavior of piles under dynamic compressive loading or horizontal loading will be the purpose of another study.
(**)8 cm spacing near pile head.
(***)f_{ck} and f_{cm}: characteristic value and average value of the concrete compressive resistance.

state is slightly changed due to the installation of the drive tube. This kind of pile has the advantage of producing little soil displacement and its use is recommended when minimum reduction of movements and soil disturbance is necessary useful or even imperative. Its use is particularly recommended when the hole is supposed to be kept stable in non-cohesive, submerged soils, etc.

2.4.2. Execution information

The steel drive tube has high resistance and a 'corkscrew' around a central hollow tube to facilitate penetration (Fig. 8).

Soil penetrated in the drive tube, under static compression, with small rotations and counter rotations, is

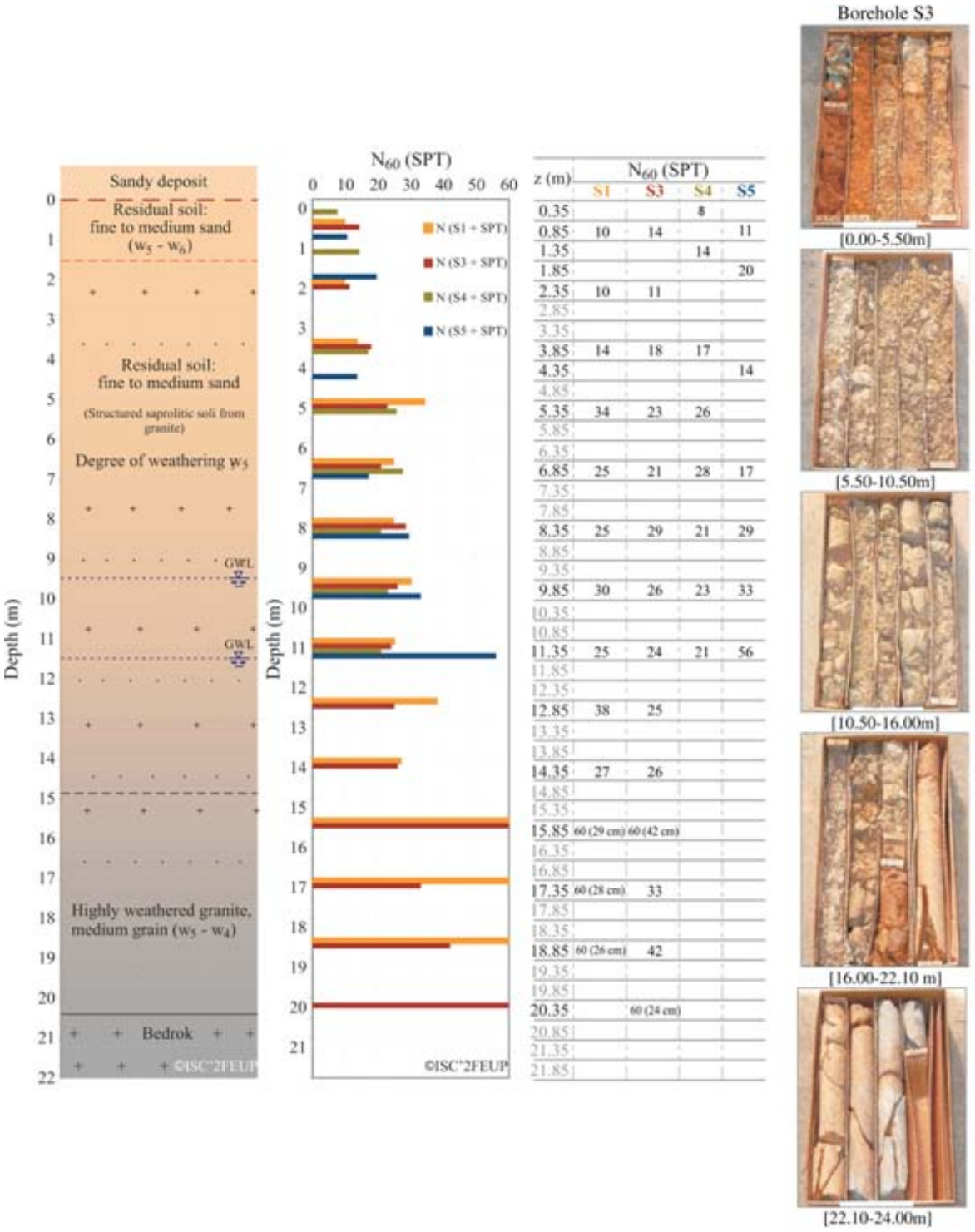

Figure 4 - Geotechnical profile and photos of the samples obtained in boreholes (Viana da Fonseca & Santos, 2008).

withdrawn by internal cleaning device, always maintaining the tube in an advanced position in relation to the borehole and cleaning device (Fig. 9). These piles are cast in place and the steel drive tube can be withdrawn or discarded after the pile is executed. In this case, it was withdrawn during the concreting process. The withdrawal process is also made by increasing static compression and tube rotation, but on a random basis, which influences pile shaft, as it can be seen in the final texture of the concrete.

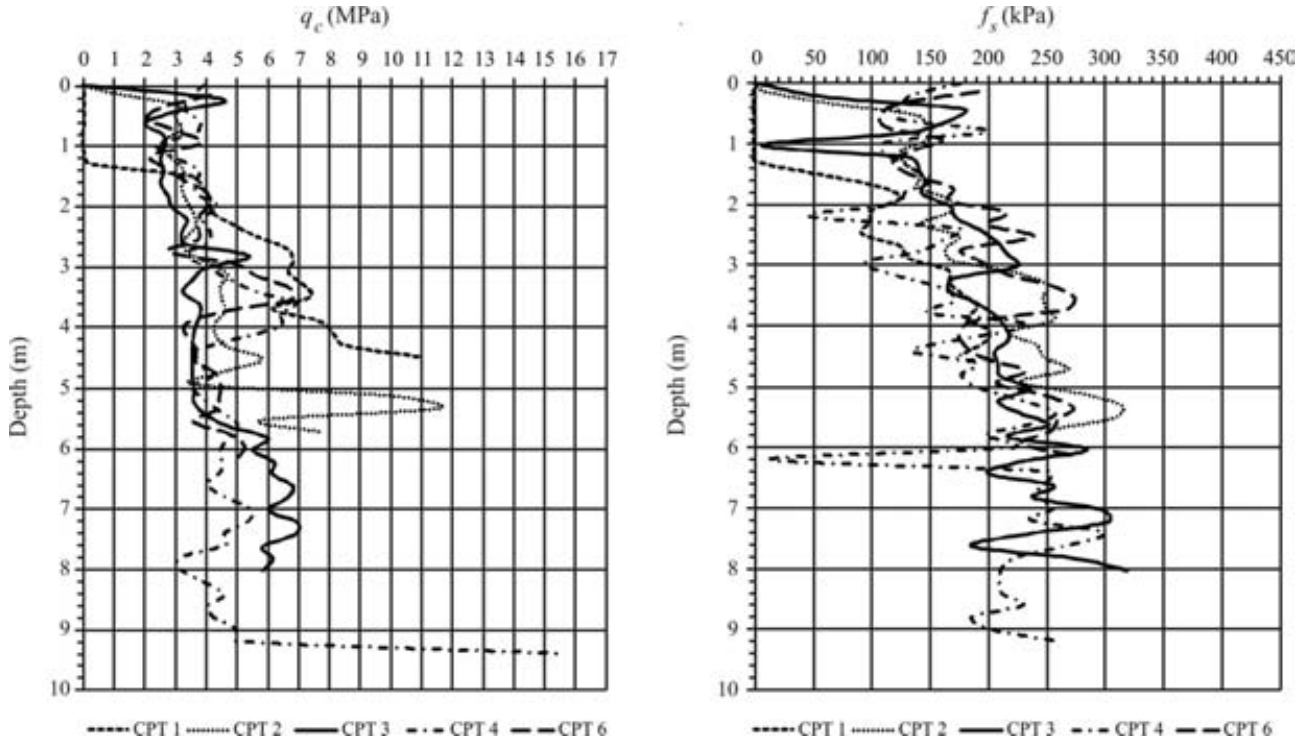

Figure 5 - Variation of q_c and f_s with depth from CPT tests (before pile execution).

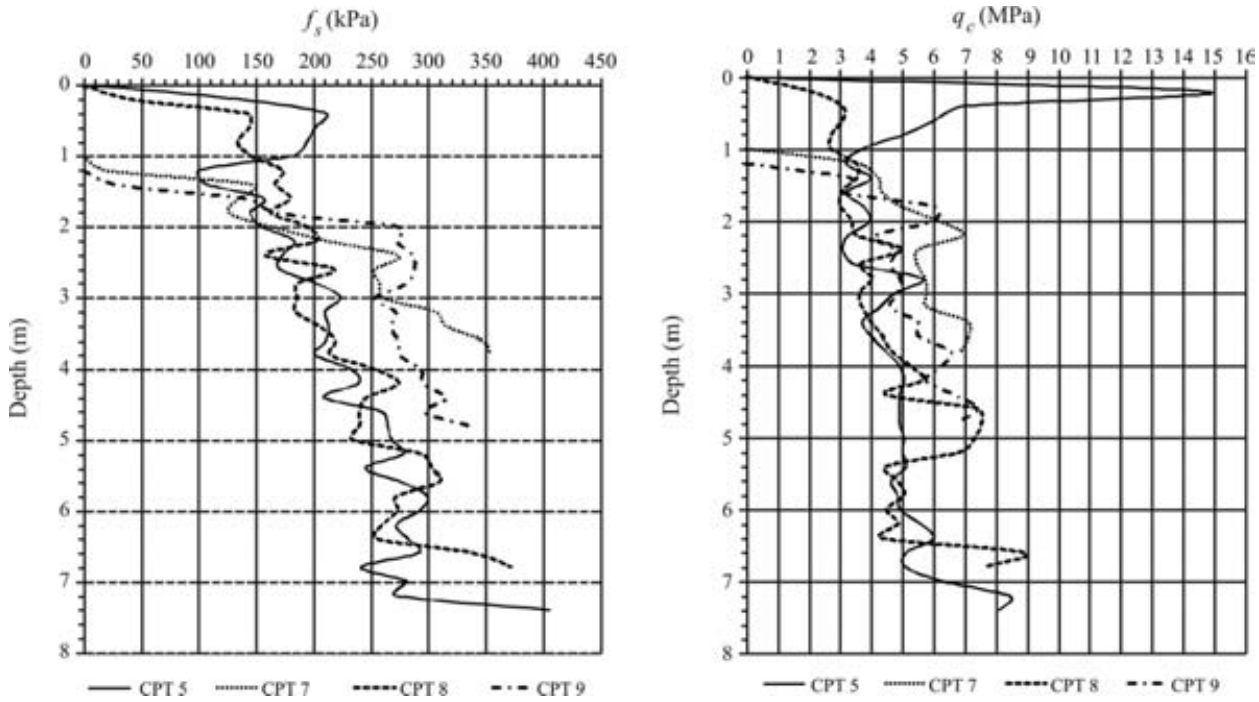

Figure 6 - Variation of q_c and f_s with depth from CPT tests (after piles execution).

As already mentioned, eight piles were used as reaction for the static loading tests; only one bored pile, E9, was tested under static compressive load, and one of these reaction piles was instrumented in order to measure lateral resistance under tension loading.

As it can be seen in Fig. 10, after removing soil from the driving tube down to a slightly higher depth (20 cm) than the final column concrete base (and with careful cleaning of the bottom), the reinforcement was installed and properly guided. Only then concreting was started, using a 'tremi' tube from the base to the top on a continuous basis

Table 2 - Load-settlement values obtained from pile load tests.

Pile	Load (kN)	Settlement (mm)
Bored – E9	900(*)	39.7
	1350(**)	155.1
CFA – T1	900(*)	10.8
	1175(**)	95.4
Precast – C1	1427	

(*)4th cycle. (**)5th cycle.

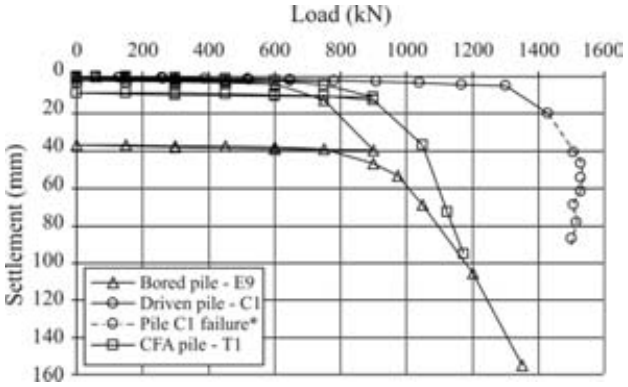

Figure 7 - Load-settlement curves from static load tests.

Figure 8 - a) and b) Steel drive tube; c) Detail of the metal drive tube base (Costa Esteves, 2005).

Figure 9 - Cleaning of the tube: a) and b) Borehole; c) Cleaning device (Costa Esteves, 2005).

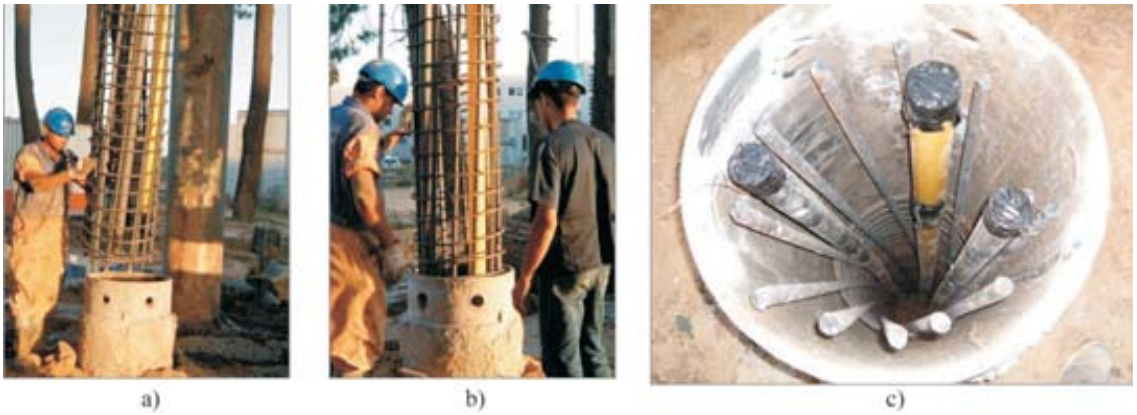

Figure 10 - a) and b) Reinforcement installation; c) Final positioning of the reinforcement (Costa Esteves, 2005).

and trying to maintain (this condition is very important) the flow of the concrete mass (Fig. 11).

2.4.3. Instrumentation

In the static axial loading tests, the load was measured using hydraulic manometers of the system and an electric load cell. Axial and transverse displacements of the pile cap were also measured in several points and with two parallel acquisition systems, assuring redundant independence which allowed to control displacements and rotations in vertical and horizontal directions, as well as the time for each measurement.

Data acquisition was automatically got with detailed temporal scanning depth.

Besides the pile cap instrumentation, six internal sensors were installed in E9 and T1 piles (Geokon *retrievable extensometer*). The sensors were inserted in PVC Hidronil tube with a 2" diameter and 6 m of length embedded in the pile. Sensors were connected to a reading unit (Geokon data logger) by an extension or electric cable from the pile cap. Figure 12 shows some details regarding the installation of the sensors and Fig. 13 shows its position in depth.

At the bottom of pile E9 a flat-jack load cell was installed with an electric cable coming up to the top of the pile to connect to the reading unit.

The load cell composed by a high resistant membrane filled with oil was placed between two 25 mm thick, 450 mm diameter steel plates. In Fig. 14b, it can be noticed that mastique was applied to avoid insertion of soil between the plates. Finally, a pressure transducer was linked to the cell (Fig. 14c).

The cell pressure measured in the static loading test multiplied with the total pile cross sectional area was assumed to correspond to the portion of applied load reaching the pile tip. In Fig. 14 (d, e, f) procedures for the installation of the already mentioned load cell are shown.

The characteristics of the pressure transducer and load cell can be seen in Table 3.

Four linear variable differential transducers (LVDT) were installed in the three studied piles with 50 mm range and 0.01 mm precision for the measurement of vertical displacements and two transducers with the same characteristics for the measurement of horizontal displacements. Simultaneously and for redundancy reasons, two mechani-

Figure 11 - a) and b) Piles concreting; c) Finalized concreting (Costa Esteves, 2005).

Figure 12 - Internal instrumentation: a) Anchor; b) Sensor c) Installation of sensors inside PVC tube; d) Sensors connections to reading unit (Costa Esteves, 2005).

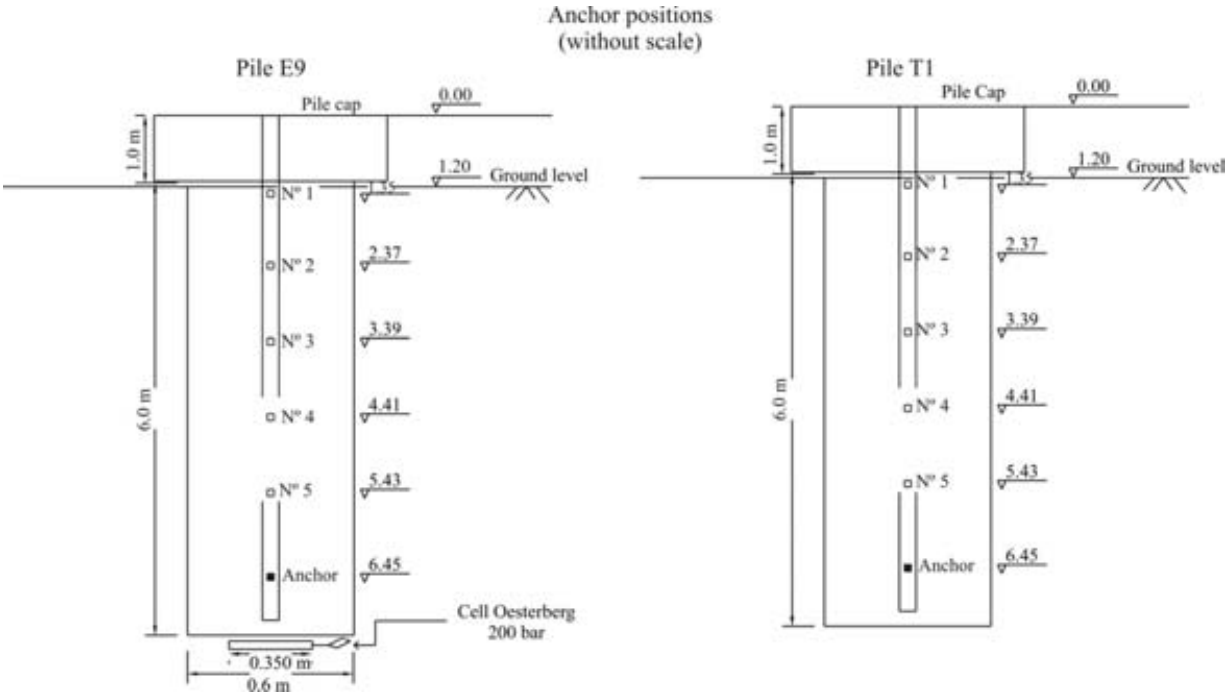

Figure 13 - Location of sensors (retrievable extensometer) (Costa Esteves, 2005).

cal dial gage devices (DG) were installed in order to check the results obtained by the electronic transducers (Fig. 15).

Converting measurements of strain to load is frequently thought to require knowledge of pile cross section and Young modulus.

The Young modulus of the pile was obtained from the slope of the strain on the instrument installed in the reference section of the pile – Level 1 (Fig. 16).

The slopes of the shortenings curves (kN/mm) are proportional to the axial stiffness, EA, of the pile. The slope corresponding to modulus value of 20 GPa is indicated under assumption that the pile diameter is equal to the nominal 600 mm value and the distance between gages points of 1020 mm.

Figure 16 shows the shortenings-load curves for each instrumented level of the bored pile.

2.5. Case 2 – CFA pile

2.5.1. Execution technique

The continuous flight auger piles (CFA) are cast in place by drilling the soil through a continuous auger, with a 'corkscrew' around a central hollow tube. After reaching the bottom level, while the auger is pulled up, the soil is replaced with concrete, pumped down through the hollow

Figure 14 - Load cell installation (Costa Esteves, 2005).

Table 3 - Load cell characteristics.

Pressure transducer		Load cell	
Type	Weight-resistivity	Plate diameter [m]	0.45
Range [MPa]	0-25	Load cell diameter [m]	0.35
Sensitivity to mA [MPa/mA]	1.5625	Load cell area [m^2]	0.096

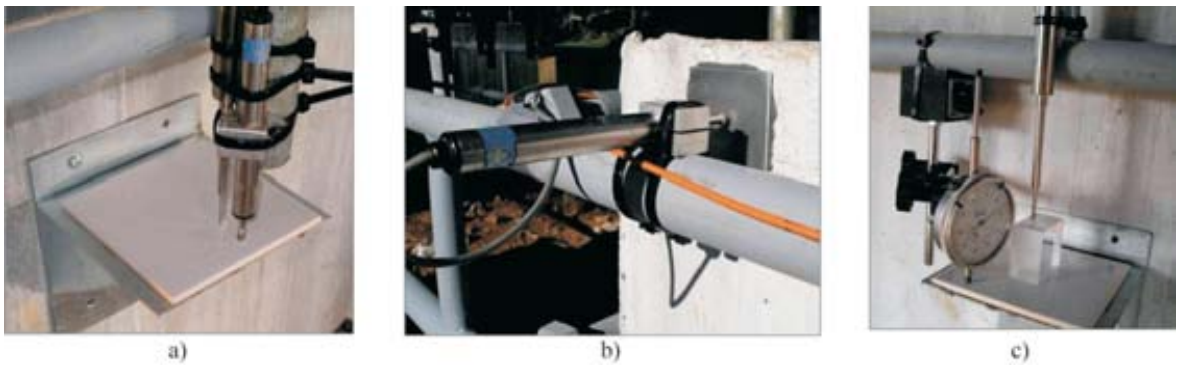

Figure 15 - Pile cap instrumentation: a) and b) LVDT transducers; c) DG devices (Costa Esteves, 2005).

tube. There is a metal cap (plug) in its bottom, which opens, like a valve, by the injected concrete to prevent soil or water from entering the hollow tube. As the auger is removed, soil confined between 'corkscrews' is also replaced by the concrete being injected from the tip level upwards. The concrete is characterized by a mixture of small aggregate and sand with cement (minimum consumption of 400 kg/m^3) and a value of slump of 190 mm, following prescriptions from The Brazilian Association of Foundations Companies Procedures Manual (ABEF, 1999). The advantages of using this type of pile are: reduced work schedule; applicability in rather diversified classes of terrains (except for rocks or soils with boulders); lack of disturbances and low vibration level in terrain, in opposition to percussion driving

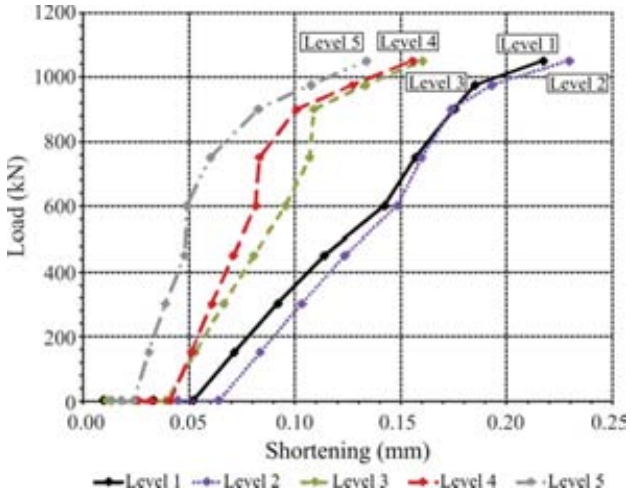

Figure 16 - Shortening-Load curves (bored pile).

techniques; and, absence of soil decompression and contamination when bentonite or other slurries are used. Disadvantages are associated to the need for a plain terrain allowing the equipment to move easily; the demand for a concrete plant close to the work; the need of a shovel loader for soil cleaning and removal, extracted during the drilling; the demand for a minimum volume of piles to justify the equipment mobilization in cost-benefit optimization; and, last but not least, the limitation of pile length and reinforcement, which may be considered determinant in certain projects. The production process must receive special attention, especially for shaft continuity control and subsoil disturbance on drilling. It is also important to observe that, in weak soils, concrete injected with high pressure may lead to soil rupture and high consumption. In these situations pressure is due to be moderate and thoroughly controlled by experience. Another important advantage of CFA piles is the possibility of continuous electronic monitoring, providing pile execution monitoring, which will be easily accessed and allow an eventual correction. The following parameters are registered: date and time; digging depth; penetration speed; torque; concrete volume and pressure; pile diameter; and pile extraction velocity.

2.5.2. Information on execution

Three CFA piles with 0.60 m diameter and 6 m depth were executed. Twelve reinforcing bars 25 mm diameter ($\cong$ 59 cm^2) and 6 m length were used. Stirrups with 10.0 mm of diameter, spaced in 10 cm completed the reinforcements. The concrete resistance (fck) was 44.0 MPa.

2.5.3. Instrumentation

In this item, the data obtained from the pile instrumentation are presented. Five retrievable extensometers were installed at depth as previously described and according to Fig. 13.

The slope corresponding to modulus value of 40 GPa is indicated under assumption that the pile diameter is equal to the nominal 600 mm value and the distance between gages points of 1020 mm.

Figure 17 shows the shortenings-load curves for each instrumented level and loading cycle.

2.6. Case 3 – Precast pile

2.6.1. Execution technique

The precast pile was installed by impact percussion and it is included in the group named 'displacement piles'. Precast piles can be made of reinforced and pre-stressed concrete compacted by vibration or centrifugation. The main disadvantage of concrete precast piles is the difficulty of adapting to unpredicted soil variations. If pile length is not carefully studied, an amendment or cut will be necessary, which will interfere on the costs and schedule for job execution. When precast, these piles cause vibrations and may cause soil compaction. They need to be reinforced in order to resist to bending moments originated from lifting and transportation, driving and lateral forces from the supported structure (Fig. 18).

2.6.2. Information on execution

Driven precast concrete piles were made under rigorous control of materials, resulting in high quality reinforced concrete. The equipment used for driving the precast piles was a 40 + 10 kN hydraulic hammer. The pile had a square cross-section (350 mm x 350 mm) and was precast down to the desired depth to an embedded length of 6 m. After driving, the pile was cut off to the desired level.

3. Analysis of Data Obtained From Instrumentation

As stated before, bored and CFA piles were instrumented along the depth, with installation of retrievable sensors. A flat-jack load cell was inserted at the bottom of the

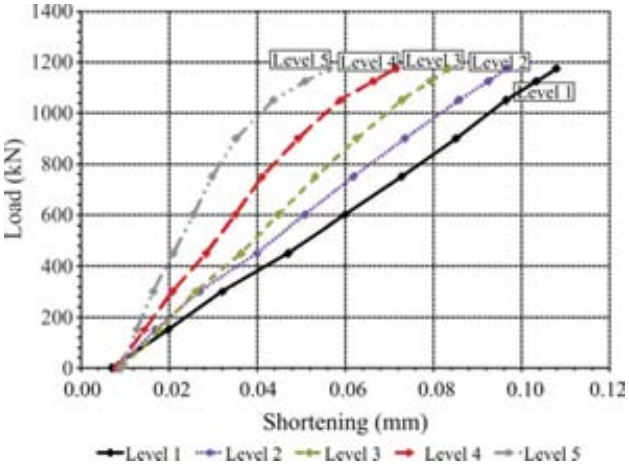

Figure 17 - Shortening-Load curves (CFA pile).

Figure 18 - Precast pile: a) Positioning b) Driving (Costa Esteves, 2005).

bored pile. The evaluation of extensometer measurements for piles E9 and T1 to load distributions indicated apparent values of shaft and tip resistances. However, residual loads were present in the piles before the static test. This effect is much more important for the driven pile C1. The analysis of axial loaded pile response can be made from diverse methods. Analysis based on soil parameters determined in laboratory or in situ tests rely on simple total stress (alpha) or effective stress (beta) methods, or on more sophisticated numerical finite element method.

The data obtained in this experimental site was analyzed by Fellenius *et al.* (2007) and Viana da Fonseca *et al.* (2007). Fellenius *et al.* (2007) used the beta-method and special preference was given to analysis based on CPTU data, for its continuous and representative scanning of the ground spatial variations. Viana da Fonseca *et al.* (2007) used a mathematical model developed by Massad & Lazo (1998) and Marques & Massad (2004), called "Modified Two Straight Lines Method" for rigid or short piles.

These analyses provided similar and consistent results regarding the mobilized lateral and tip resistances. For the bored and CFA piles the maximum load at each pile head are from a settlement of about 100 mm, chosen to ensure that both piles are evaluated at the same pile settlement. Table 4 summarizes the values obtained by Fellenius *et al.* (2007) and Viana da Fonseca *et al.* (2007).

The estimated unit shaft resistance was about 60 kPa and the applied load reaching the bored and CFA piles tip was 42%. The driven pile although having a smaller cross-section (43.3%) showed a stiffer response and higher resistance than the other two piles, which are a clear indication of installation effects and its importance in the pile response.

4. Evaluation of Piles After Removal of Soil

In order to inspect the geometrical characteristics of the executed piles and to confirm their integrity, phased excavation of the soil around the piles was carried out, aiming not only at obtaining a good visual characterization but also successive samples of blocks for laboratory testing. This was done up to approximately 6 m depth. For this removal, a study had to be conducted on the possible ways of extraction, since this is a complex and expensive process. Following, all the excavations steps are described.

To remove the piles, it was necessary, as already mentioned, to excavate the surrounding soil. This excavation should be phased, not only to avoid risks associated with instability of excavation ramps but also to enable pile removal with minimum possible damage.

For pile removal, the selection of the retro-excavator to be used (arm length and capacity) was carefully made, considering the weight and the length of all elements (piles and cap block). In Fig. 19, the beginning of excavation is shown with the chosen retro-excavator, with a 6 m length arm.

Two distinct situations were considered in this process: one regarding the removal of the 6 m long piles and the other removal of 22 m long piles to avoid any interference with future constructions in the area. Although it would be interesting to remove all the piles, this was not considered necessary, since the deepest objects would not affect future constructions. Thus, the 6 m long piles were removed as a whole while the others were cut-off approximately at the 5 m portion (from soil level) and then removed. Figure 20 shows the schematic procedure utilized to remove the 6 m long piles and Fig. 21 shows the adopted procedure for the 22 m long piles.

After pile removal, relevant geometrical characteristics were measured after properly cleaning the piles from existing soil in the shaft length. It was observed that geometrical characteristics for bored and CFA piles diameters

Table 4 - Load Distribution for 100 mm pile head settlement.

Pile	Viana *et al.* (2007)			Fellenius *et al.* (2007)		
	Q_l (kN)	Q_p (kN)	Total load (kN)	Q_l (kN)	Q_p (kN)	Total load (kN)
E9 (Bored)	696	481	1177	700	500	1200
T1 (CFA)	703	499	1202	700	500	1200
C1 (Precast)	511 to 1021	1004 to 494	1515	520	980	1500

Figure 19 - Excavation: a) beginning of job; b) c) steps for soil removal (Costa Esteves, 2005).

Figure 20 - Pile extraction (6 m): a) beginning of excavation; b) and c) and d) removal of pile from the soil; e) transportation of pile to the warehouse; f) general view of the pile after removal (Costa Esteves, 2005).

were slightly higher than the initial nominal diameter (605 mm and 611 mm, respectively).

It is important to highlight that the shaft surface of CFA piles was smoother than the bored pile executed with temporary casing (Fig. 22) and that the last 20 cm to 30 cm of the bored piles showed a significantly reduced diameter, reaching 12% of reduction in pile E9 (525 mm), as it can be seen in Fig. 23.

As reported in item 2.4.2, removal of drive tube in bored piles is made by ascending static pressure and tube rotation, but on a random basis, which does not promote a perfectly smooth shaft texture in bored piles, as shown in Fig. 22.

This study on pile removal also enabled to check conditions of the load cell utilized at the base of pile E9. The load cell was well positioned at the pile base, as seen in Fig. 24.

5. Comparison with Results Obtained in the EF-Unicamp

Based on the results presented in Part 1 of this paper, the following observations are made:

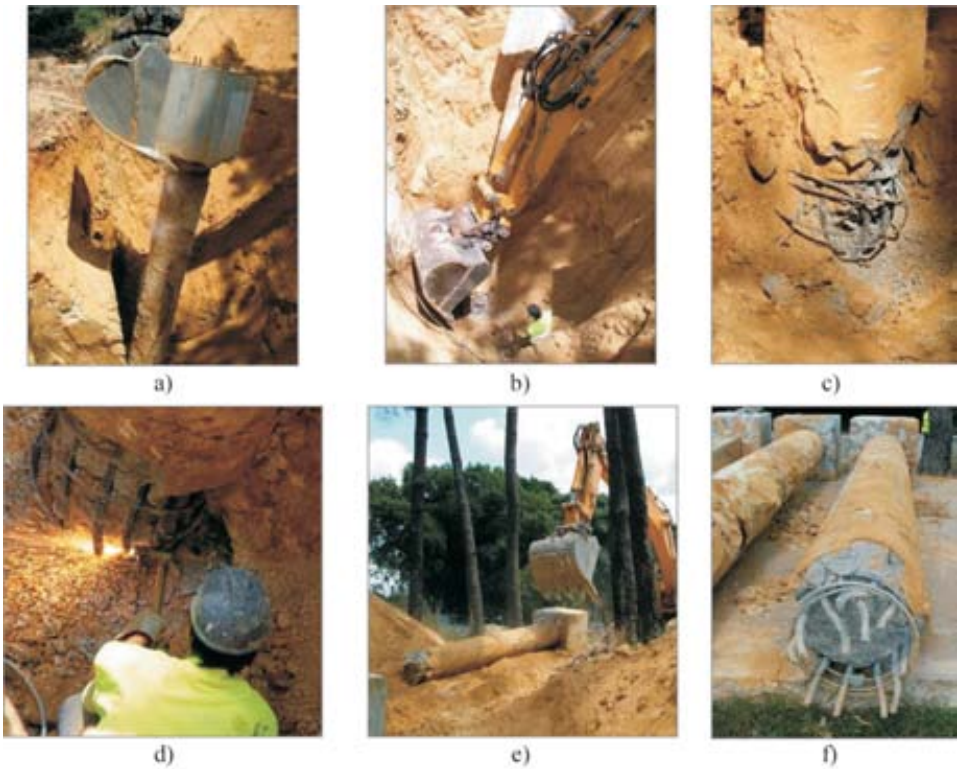

Figure 21 - Pile extraction (22 m): a) and b) pile cut-off at portion 5 m; c) and d) detail of the cut pile e) removal of pile from the soil; f) general view of the pile after removal from the soil (Costa Esteves, 2005).

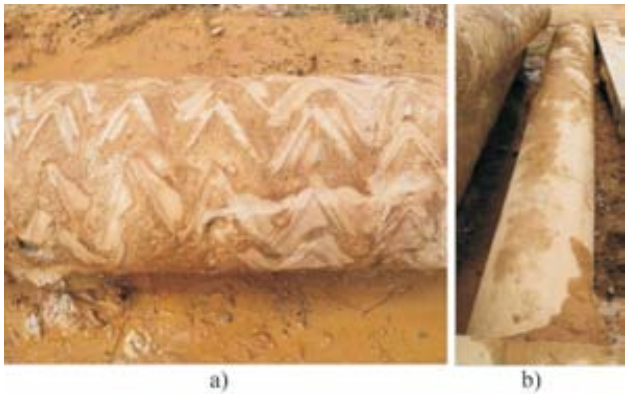

Figure 22 - Detail of pile shaft texture: a) bored; b) CFA (Costa Esteves, 2005).

As for piles executed at the Experimental site of FEUP, it was found that, unlike pile behavior at the Experimental site of Unicamp, the tip of the piles absorbed high loads of around 29% for bored and CFA piles, at Unicamp the average values were about 2% and 7% for bored and CFA piles.

This difference between the values obtained for load absorption at the tip in both experimental fields is explained by the difference between the two soils, which have distinct genesis and resistance. While the pile tip region at the Experimental Site of Unicamp has N_{SPT} average values of 10 blows and cone resistance of 2 MPa, in the EF-FEUP, average N_{SPT} values of 25 blows and cone resistance of 4 MPa are found.

Figure 23 - Bottom of the bored pile E9 (Costa Esteves, 2005).

In the site of EF-FEUP, both CFA and bored piles behaved similarly in terms of lateral friction. The same happened to the CFA and bored piles in the EF-Unicamp.

Two different techniques were utilized for instrumentation of pile shafts; the process executed by Unicamp researchers was a rather 'handicraft' one, while the one used by FEUP's researchers utilized electric removable extensometers manufactured by a specialized company. Equipment installation techniques on piles were very similar, *i.e.*, from insertion of the tube in piles. In spite of utilizing distinct techniques, it was observed that both techniques are

Figure 24 - Load cell and the pile base (Costa Esteves, 2005).

good in terms of measuring load distribution in a deep foundation.

6. Conclusions

From the assessment of results obtained from the performed tests, the following conclusions can be drawn:

Based on the results obtained from the bored and CFA piles, it seems that the execution process of CFA pile did not provide differences on behavior regarding shaft resistance of this type of foundation, which means, it behaved as a bored pile.

Regarding the tip resistance results obtained from CFA and bored piles, both showed similar values, but soil on CFA pile tip was less disturbed, while in the bored pile the soil gradually became stiffer as successive loadings occurred.

After the loading tests the piles were extracted and inspected. The pile surfaces were smooth and the actual diameter of piles was very close to the nominal value.

Evaluation of extensometer measurements for piles E9 and T1 to load distributions indicated values of shaft and tip resistances. However, residual loads were present in the piles before the static test, for which the actual magnitude was estimated after trial-and-error back-analysis. The estimated unit shaft resistance was about 60 kPa and the applied load reaching the pile tip was 42%.

The precast pile C1 although having a smaller cross-section showed a stiffer response and higher resistance than the other two piles. This is a clear indication that the installation effects play an important role in the pile behavior. In this case, the pile driving process should have induced significant changes in the surrounding soil affecting the shaft resistance and inducing residual loads.

References

American Society of Civil Engineers (ASTM) (1994) D 1143-81: Piles under static axial compressive load. Standard test method. In: Annual Book of ASTM Standards, Philadelphia, v. 04.08, pp. 96-106.

Associação Brasileira de Empresas de Fundações (ABEF) (1999) Manual de Especificações de Produtos e Procedimentos, 2ª ed. ABEF, São Paulo, 282 pp.

Associação Brasileira de Normas Técnicas (ABNT) (1992) NBR 12131: Estacas: Prova de Carga Estática. Rio de Janeiro.

Costa Esteves, E. (2005) Ensaios e Análise de Resposta de Estacas em Solo Residual do Granito sob Acções Verticais. MSc Thesis, Faculdade de Engenharia, Universidade do Porto, Porto, 322 pp.

De Cock, F.; Legrand, C. & Huybrechts, N. (2003) Axial static load test (ASPLT) in compression or in tension – Recommendations from ERTC3-Piles, ISSMGE Subcommittee. Proc of the XIII ECSMGE, Prague. v. 3, pp. 717-741.

Fellenius, B.H.; Santos, J.A. & Viana da Fonseca, A. (2007) Analysis of piles in a residual soil – The ISC'2 prediction. Canadian Geotechnical Journal, v. 44, p. 201-220.

Marques, J.AF. & Massad, F. (2004) Provas de carga instrumentadas com bulbos, executadas na região praieira de Maceió, Alagoas. Solos e Rochas, v. 27:3, p. 243-260.

Massad, F. & Lazo G. (1998) Método gráfico para interpretação da curva carga-recalque de provas de carga verticais em estacas rígidas ou curtas. Anais do XI Congresso Brasileiro de Mecânica dos Solos e Engenharia Geotécnica, Brasília, v. 3, pp. 1407-1414.

Viana da Fonseca, A.; Carvalho, J.; Ferreira, C.; Tuna, C.; Costa Esteves, E. & Santos, J.A. (2004) Geothecnical characterization of a residual soil profile: the ISC'2 experimental site. Proc. ISC'2 Geothecnical and Geophysical Site Characterization, Rotterdam, v. 2, pp. 1361-1369.

Viana da Fonseca, A.; Santos, J.A.; Costa Esteves, E. & Massad, F. (2007) Analysis of piles in residual soil from granite considering residual loads. Soils and Rocks, v. 30:1, p. 63-80.

Viana da Fonseca, A. & Santos, J.A. (2008) International Prediction Event. Behaviour of Bored, CFA and Precast Piles in Residual Soil. ISC'2 Experimental Site. University of Porto and Tech. Univ. of Lisbon, Porto and Lisbon, 699 pp.

Evaluation on the Use of Alternative Materials in Geosynthetic Clay Liners

P.M.F. Viana, E.M. Palmeira, H.N.L. Viana

Abstract. Geosynthetic clay liners (GCL) have been increasingly used in barrier systems of waste disposal areas and in hydraulic works. However, sometimes they are discarded as possible barrier solutions in these works because of their greater costs in comparison with other solutions (geomembranes or compacted clay liners). This paper presents a laboratory study to investigate the technical feasibility of mixing alternative materials to bentonite for the production of alternative low cost GCLs. The alternative materials used were sand, clay and tire grains. Direct shear, consolidation, and expansibility tests were carried out on bentonite mixtures with varying percentages in mass of the alternative material. Ramp tests and expansibility tests were also performed on alternative GCLs manufactured with these types of mixtures. The results obtained showed that the presence of the alternative materials in the bentonite increased the shear strength and the permittivity of the mixture and reduced its expansibility. The tests on the bentonite-tire grains mixtures suggest that alternative GCLs manufactured with this type of mixture may be used in less critical barrier systems (particularly under high stress levels) and as bedding/protective layers underneath geomembranes, also providing a better use for wasted tires in environmental terms.

Keywords: GCL, alternative materials, laboratory tests, ramp tests.

1. Introduction

Geosynthetic Clay Liners (GCLs) are relatively thin geosynthetic products used as barriers in hydraulic and waste disposal works. They consist of a layer of bentonite enveloped by geosynthetic layers (usually geotextiles). Variations are possible, like products consisting of a layer of bentonite on a geomembrane (Koerner, 2005).

The use of GCLs as barriers in environmental protection projects has increased markedly in the last decade, mainly due to its low hydraulic conductivity (typically $\leq 10^{-11}$ m/s), easy and quick installation, self-healing capacity in case of damage during installation and good overall performance. Several works can be found in the literature reporting successful applications of GCL in environmental protection works (Reuter & Markwardt 2002, Didier & Nassar 2002, Rowe & Orsini 2003 and Shan & Chen 2003, Touze-Foltz *et al.*, 2006).

Hydraulic conductivity is a major factor to be considered when using GCLs in hydraulic and environmental projects. The low permeability of the bentonite guarantees a satisfactory performance as a barrier if damages during transport of the product to the job site and installation are avoided or minimised. In this sense, the self-healing capacity of GCLs is a great advantage in comparison to other barrier systems. Shan & Daniel (1991) and Sivakumar Babu *et al.* (2001) have shown that cracks in a GCL, as a consequence of a dry period, were closed in a subsequent wetting period, without compromising its barrier function. Expansion of the GCL due to hydration may increase its thickness significantly, depending on the stress level on the GCL, reducing even further its permittivity. Permittivity (ψ) values of GCLs are typically lower than 10^{-9} s^{-1}.

Besides low hydraulic conductivity and self-healing capacity, the internal shear strength of GCLs products is of utmost importance in the design of lining systems on slopes, because of the low shear strength of bentonite, particularly when hydrated. The internal shear strength of a GCL depends on the bentonite shear strength and on the strength of the fibres used to fix its cover and carrier layers, as well as on the manufacturing process used (stitching or needle-punching). Chiu & Fox (2004), Fox & Stark (2004) and Viana & Palmeira (2009) discussed the importance of the internal shear strength of GCLs and how it can be severely reduced due to hydration. However, the internal shear strength of GCL products can be markedly increased depending on how they are manufactured and on the mechanical strength of the fibres used to fix the geotextile cover layers (Bouazza, 2002, Bouazza & Vangpaisal, 2007, Müller *et al.*, 2008).

Some materials can be mixed to the bentonite as a way to reduce the GCL cost, improve some of its relevant properties and, in the case of waste materials, to provide a better and more environmentally friendly destination of such materials (Viana & Palmeira 2008, Viana & Palmeira 2009, Ikizler *et al.* 2009). For instance, the mixture of fine sand to the bentonite can increase its internal shear strength and resistance against perforations and cuts, without compromising its low hydraulic conductivity. However, the manufacturing process and costs may be influenced by the presence of sand mixed to the bentonite. Besides, the

P.M.F. Viana, DSc., Associate Professor of Civil Engineering, Departamento de Engenharia Civil, Universdade de Goiás, Anápolis, GO, Brazil. e-mail: paulo.viana@ueg.br.
E.M. Palmeira, PhD., Professor of Civil Engineering, Departamento de Engenharia Civil e Ambiental, Universidade de Brasília, Brasília, DF, Brazil. e-mail: palmeira@unb.br.
H.N.L. Viana, DSc., Geotechnical Engineer, Secretaria de Infra-Estrutura Hídrica, Ministério da Integração Nacional, Brasilia, DF, Brazil.
Submitted on May 17, 2010; Final Acceptance on November 3, 2010; Discussion open until August 31, 2011.

expansibility, and by so the permittivity, of the alternative GCL may be affected because of the addition of a non expansive material and this should be properly evaluated.

This paper examines the influence of adding non conventional materials to bentonite to form alternative and low cost GCLs and the repercussion of the addition of these materials on the hydraulic and strength properties of the GCLs. Two commercially available conventional GCLs were used as references for comparisons. Small and large scale laboratory tests were performed in this study and the experimental methodology and results obtained are presented and discussed in the following sections.

2. Experimentals

2.1. Materials used in the experiments

2.1.1. Bentonite

A sodic bentonite (code BTN), produced by Bentonit Nordeste Ltd., Brazil, was used in the tests and its main properties are summarized in Table 1. X rays diffractometry tests showed that the bentonite was predominantly composed by sodium montmorillonite with some illite, calcite and quartz.

2.1.2. Materials used in the bentonite mixtures

Three materials were mixed to the bentonite (BTN) to form the alternative GCL products. These materials were a fine sand (code SND), a clay (kaolinite, code CLY) and tire grains (code TG) from wasted automobile tires. Table 2 presents the main properties of these materials. Figure 1 shows views of the materials mixed to the bentonite.

Table 1 - Physical properties of the bentonite used in laboratory testing.

Grain unit weight (kN/m^3)	26.60
Liquid limit (%)	381.0
Plastic limit (%)	133.0
Plasticity index (%)	248.0
Initial water content (%)	14.0%
Minimum dry unit weight (kN/m^3)	7.3

*Chemical composition: 60.2% de SiO_2, 18.5% Al_2O_3, 7.2% Fe_2O_3, 2,5% de Na_2O, 2.4% de CaO, 2.0% MgO e 0.53% K_2O.

2.1.3. GCLs tested

Two commercially available GCLs (codes GCLA and GCLB) manufactured with sodic bentonite and three

Table 2 - Physical properties of the materials used in the tests.

Property	Sand	Clay	Tire grains
D_{10} (mm)[1]	0.08	0.02	0.12
D_{60} (mm)	0.25	0.07	0.48
D_{85} (mm)	1.00	0.08	0.60
Particle unit weight (kN/m^3)	26.8	28.2	11.5
CU[2]	3.10	3.50	4.0
Friction angle (degrees)	34[3, 4]	34.1[6]	23[3,7]
Cohesion (kPa)	-	6.14[5,6]	-
Maximum void ratio	0.93	-	-
Minimum void ratio	0.63	-	-
Liquid limit (%)	-	36	-
Plastic limit (%)	-	26	—
Optimum moisture content (%)[8]	-	23	—
Maximum dry unit weight (kN/m^3)[8]	16.3	14.9	4.9
Percentage of carbon (%)	-	-	> 80

Notes: (1) D_n - diameter for which *n*%, in mass, of the remaining soil particles are smaller than that diameter; (2) Coefficient of uniformity (= D_{60}/D_{10}); (3) Friction angle obtained in direct shear tests for a stress level ranging from 15 kPa to 200 kPa (4) For a sand unit weight of 16.3 kN/m^3; (5) From drained direct shear tests for a stress level ranging from 15 kPa to 200 kPa; (6) Under optimum moisture conditions (clay dry unit weight of 14.9 kN/m^3); (7) For a tire grains unit weight of 4.9 kN/m^3; (8) Normal Proctor compaction energy.

Figure 1 - Materials mixed with the bentonite to produce the alternative GCLs: (a) Tire grains (TG); (b) Sand (SND) and (c) Clay (CLY) - 50x enlargement.

alternative GCLs with cores consisting of mixtures of bentonite with sand, clay or tire grains were tested. The alternative GCLs had cores consisting of 50% (in mass) of the alternative material (sand – code GCL-SND, clay – code GCL-CLY or tire grains – code GCL-TG). This percentage of alternative material was adopted based on results of tests performed with varying percentages of alternative materials that will be presented and discussed later in this paper. Table 3 summarises the main properties of the GCLs tested.

The alternative GCLs using cores with different mixtures of bentonite, sand, clay and tire grains were manufactured in the laboratory. Woven and a nonwoven geotextiles, whose main properties are listed in Table 4, were used as carrier and cover layers of these GCLs, as in conventional products. The geotextiles were stitch-bonded to form the GCL with 25 mm spacing between stitch-bonding rows, as shown in Fig. 2. Initially, a study on the influence of the stitching process was carried out, with products being manufactured with spacing between stitches equal to 2 mm, 4 mm and 8 mm. Based on this study, the 8 mm spacing was adopted for the manufacture of the GCL specimens that were subjected to expansibility and inclined plane tests.

2.2. Equipment used in the experimental programme

2.2.1. Expansion test cells

Free expansion tests on bentonite-alternative materials and on alternative GCLs were carried out for the evaluation of the influence of the type of bentonite mixture used on the product's expansibility potential. Figure 3 shows the equipment used in these tests. Each GCL specimen, 100 mm in diameter, was accommodated in the testing cell with natural moisture content. The specimen was then inundated for 96 h without any confinement and its vertical expansion was measured with dial gauges until readings stabilisation.

2.2.2. Consolidation and hydraulic conductivity tests

Consolidation and hydraulic conductivity tests under confinement on bentonite mixtures and on the alternative materials described above were performed using a standard soil consolidation testing cell. The GCL specimens were 75 mm in diameter, 20 mm thick and during the tests were subjected to normal stresses up to 200 kPa. Initially, the specimens were hydrated under a vertical stress of 5 kPa for 48 h. This period of time was adopted based on results from preliminary tests that showed that to be sufficient for mixture expansion stabilisation. After specimen expansion had been completed, the loading stages were applied, as in conventional one-dimensional soil consolidation tests. At the end of each loading stage the hydraulic conductivity of the mixture was assessed by performing a variable water head test using ports connected to the cell ends.

Table 4 - Properties of the geotextiles of the GCLs.

Property	Woven	Nonwoven
Polymer type	Polypropylene	Polypropylene
Mass per unit area (g/m^2)	110	350
Tensile strength (kN/m^2)(1)	10/10(2)	17/14(2)
Filtration opening size (μm)(3)	NA(5)	1.2×10^{-5}
Permittivity (s^{-1})(4)	NA	1.31

Notes: (1) Wide-strip tensile tests according to ASTM D4595; (2) Number on the left is the tensile strength along the warp direction while number on the right is the tensile strength along the weft direction; (3) According to NF EN ISO 12956; (4) According to ASTM D4491; (5) Not available.

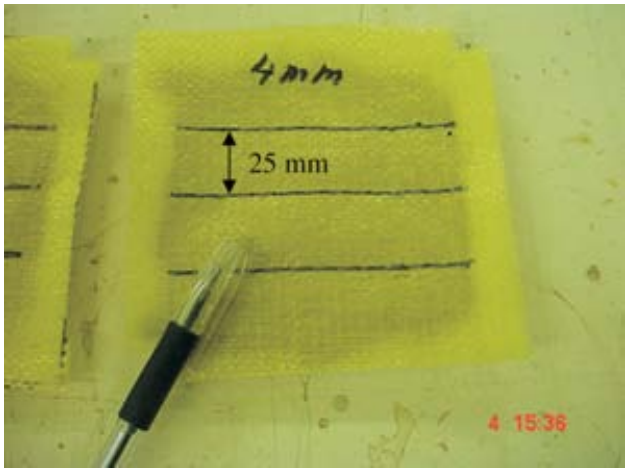

Figure 2 - Alternative GCL product.

Table 3 - Properties of the GCLs used in the tests.

Property	GCLA	GCLB	GCL-SND	GCL-CLY	GCL-TG
Bentonite type	sodic	sodic	sodic	sodic	sodic
Core dry minimum density (kN/m^3)	7.3	7.3	10.6	9.2	6.1
Thickness (mm)	6-7	6-7	6-7	6-7	6-7
Mass per unit area (g/m^2)	5000	4500	6858	5948	3965
Moisture content (%)	13.6	13.4	12.7	12.7	8.6
Manufacturing process	Stitch bonded	Needle punched	Stitch bonded	Stitch bonded	Stitch bonded

Note: The percentage (in mass) of sand, clay and tire grains in GCL-SND, GCL-CLY and GCL-TG, respectively, was equal to 50%.

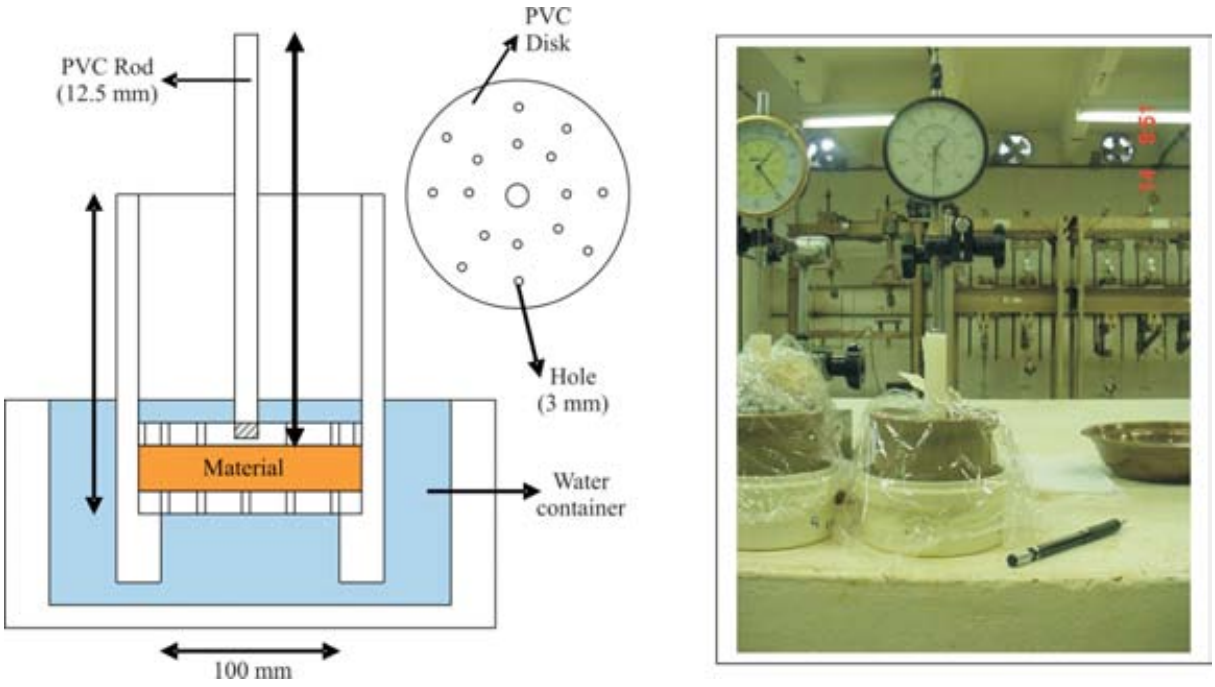

Figure 3 - Free expansion test apparatus.

2.2.3. Direct shear tests

Conventional direct shear tests were performed on the bentonite mixtures used in the experimental programme. The dimensions of the specimens tested in the conventional direct shear apparatus were 100 mm x 100 mm. Dry (under natural moisture content) bentonite mixtures were tested under minimum dry unit weight condition (loosest state) using a test speed of 0.3 mm/min. Tests on hydrated mixtures were also carried out after a period of 48 h of specimens submersion in water. A test speed of 0.03 mm/min was used for the hydrated specimens (ASTM D 6243). Vertical stresses up to 200 kPa were applied to the specimens during the tests and the procedure used was that used in conventional soil direct shear tests. Post-test investigations included assessing the shear zone at the specimen mid-height. Figure 4 shows the region of the shear zone in one of the specimens after the end of the test.

2.2.3. Ramp tests

The ramp (inclined plane) test equipment used (Fig. 5) is capable of testing GLC specimens with dimensions up to 0.6 m x 2.2 m. In this equipment the specimen can be fixed to the ramp along its entire length or to have one end anchored to the ramp (Palmeira *et al.* 2002, Palmeira & Viana 2003, Palmeira 2009, Viana & Palmeira 2010). The latter case was the one adopted in the present work. In the series of tests described in this work the dimensions of the specimens tested were 0.6 m (width) x 1.0 m (length). Tests with normal stresses up to 10 kPa were carried out. The interface between the GCL specimen and the smooth metal ramp surface was lubricated with double layers of plastic films and grease to minimise friction along this interface. Concrete blocks accommodated in a rigid box were used to provide vertical stresses on the GCL specimen. Displacement transducers allowed for the measurement of the displacements of this box during the tests and a load cell fixed to the anchored GCL end measured the tensile forces mobilised in the specimen. In these tests the upper geotextile layer was cut and only the bottom one (carrier layer) was anchored to the ramp extremity. This procedure was adopted to favour internal failure of the GCL. Tests on dry and on hydrated GCL specimens were carried out. For the latter case a water filled container was installed on the ramp for the hydration of the specimen prior to testing.

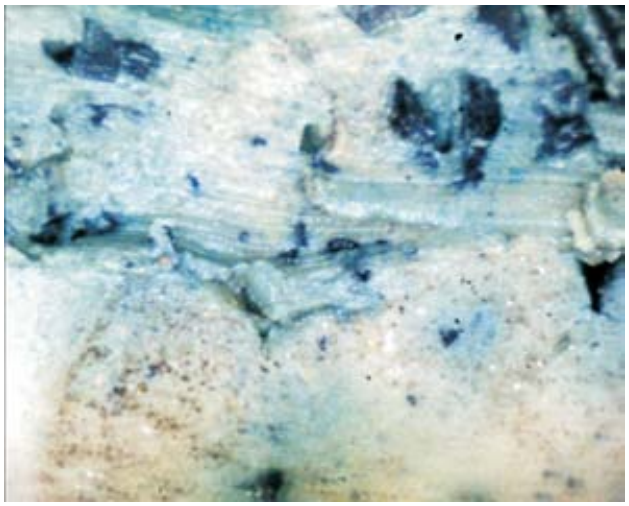

Figure 4 - Shear zone region in a test on GCL-TG 50% (50% in mass of tire grains) at the end of a direct shear test.

Figure 5 - Large scale ramp test equipment.

3. Results Obtained

3.1. Tests on bentonite mixtures

Direct shear, expansion and consolidation tests were performed in the mixtures of bentonite with sand, clay or tire grains for percentages (in mass) of these materials in the mixtures equal to 25%, 50% and 75%. Tests on each individual material were also carried out and their results were used as references for comparisons.

3.1.1. Direct shear tests

Figures 6(a) to (c) shows typical shear stress – shear displacement curves obtained in conventional direct shear tests (100 mm x 100 mm specimens) carried out on "dry" (natural moisture content) bentonite mixtures, containing 50% of the alternative material in mass, under a normal stress of 100 kPa, as well as results of tests on each individual component of the mixture. Table 5 shows the initial conditions of the specimens in terms of moisture contents and void ratios. The mixture specimens were prepared under the loosest stated possible by gently placing the mixture in the testing cell (no compaction). The results in Fig. 6 show the beneficial aspects brought by the presence of the alternative material to the increase of the shear strength of the mixture. The presence of these materials reduced the mixture void ratio, increasing the shear strength of the mixture. This increase is more clearly visualised at later stages of the tests on the BTN-SND and BTN-CLY mixtures (Figs. 6a and 6b). Regarding the BTN-TG mixture, gains of shear strength with respect to test on the bentonite alone only occurred after large shear displacements (above 5 mm, Fig. 6c). This was in part due to the compressibility and to the greater values of initial void ratios of the mixture with tire grains.

Figure 7 summarises the results of friction angles of the dry bentonite mixtures obtained in the direct shear tests. In this figure, R_ϕ is the ratio between the tangent of the mixture friction angle and the tangent of the friction angle of the bentonite alone. It can be noted that R_ϕ tends to increase with the increase of the percentage of the alternative material in the mixture, with greater gains in friction angle for the BTN-SND and BTN-CLY mixtures. The presence of a coarser material mixed with bentonite will provide greater strength along the shear plane. This can be observed in Fig. 8, which shows views (50x enlargement) of shear zones at the end of tests on hydrated BTN-TG mixtures for percentages of tire grains of 25%, 50% and 75%. It is interesting to note the reduction on the value of R_ϕ for the test on the tire grains alone (R_ϕ = 0.7) in Fig. 7. This was due to the large value of void ratio (e = 4.6) of the tire grains specimen, as shown in Table 5.

Very low values of cohesion intercept were obtained in direct shear tests on dry bentonite mixtures. These intercepts were negligible for BTN-SND and BTN-TG mixtures. For BTN-CLY mixtures it varied between 0 and 6.1 kPa, depending on the percentage of clay in the mixture.

Figure 9 presents values of mixture friction angle and R_ϕ obtained in conventional direct shear tests on hydrated (after 4 days under submersion) specimens. In general,

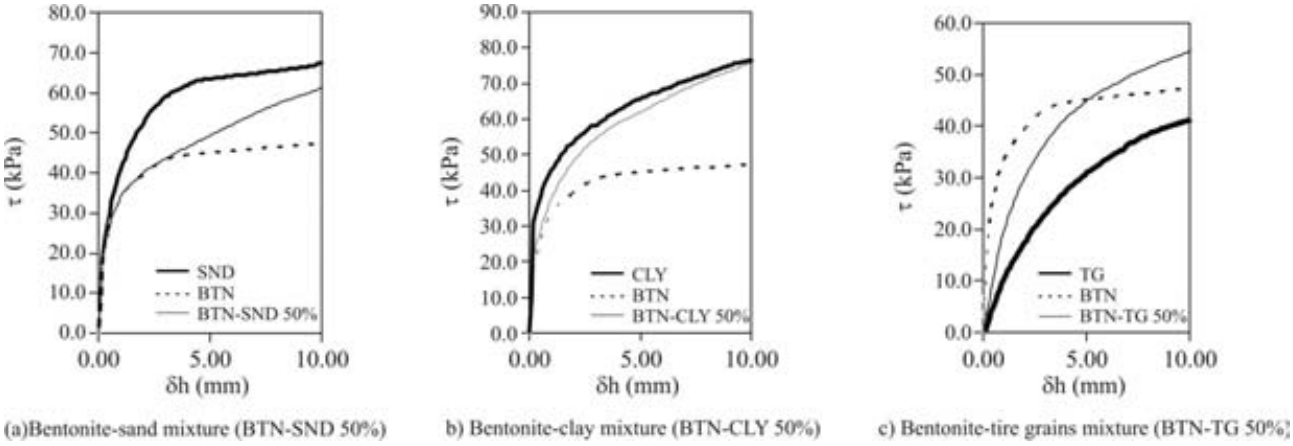

Figure 6 - Typical shear stress-shear displacement curves obtained in tests on bentonite mixtures containing 50% (in mass) of bentonite.

Table 5 - Moisture content and void ratio of the mixtures tested.

Material	% of BTN (%)	$w_i^{(1)}$ (%)	w_{4d} (%)	e_o	e_{4d}
BTN	100	12	139	3.3	7.5
CLY	0	1	57	1.2	1.2
SND	0	0	22	0.9	0.9
TG	0	1	40	4.6	4.6
BTN-CLY 25%[(2)]	75	10	123	3.1	7.3
BTN-CLY 50%	50	8	123	2.8	6.5
BTN-CLY 75%	25	8	103	2.6	5.6
BTN-SND 25%	75	11	117	2.8	6.3
BTN-SND 50%	50	10	112	2.5	5.6
BTN-SND 75%	25	7	107	1.9	3.5
BTN-TG 25%	75	10	123	3.2	7.3
BTN-TG 50%	50	9	111	3.0	7.3
BTN-TG 75%	25	6	79	2.9	5.1

Notes: (1) w_i = natural moisture content, w_{4d} = moisture content after 4 days of inundation, e_o = initial void ratio, e_{4d} = void ratio after 4 days of inundation; (2) Number on the right indicates the percentage of alternative material, in mass, mixed to the bentonite.

hydration caused a drastic reduction on mixture friction angles. The low friction angle obtained in the test with the bentonite alone is consistent with values reported in the literature (Fox *et al.* 1998, Thiel *et al.* 2001, Fox & Stark 2004, Viana & Palmeira 2009). A more significant increase on R_ϕ was observed for the mixture BTN-TG with a percentage of tire grains greater than 50%. In spite of the reduction of the friction angle caused by hydration, the addition of alternative material led to greater shear strength of the mixture in comparison to that of the bentonite alone.

The variation of the cohesion intercept with the percentage of alternative material in the mixture obtained in the direct shear tests on hydrated specimens is depicted in Fig. 10. It can be noted that the cohesion intercept decreases from the value (~12 kPa) obtained for the bentonite alone with the increase of mass of alternative material. For values up to 75% of alternative material in the mixture, the cohe-

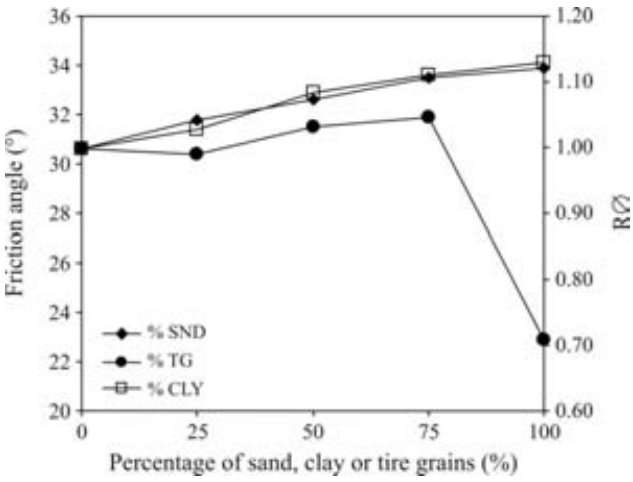

Figure 7 - Bentonite mixture friction angles for different percentages of alternative materials.

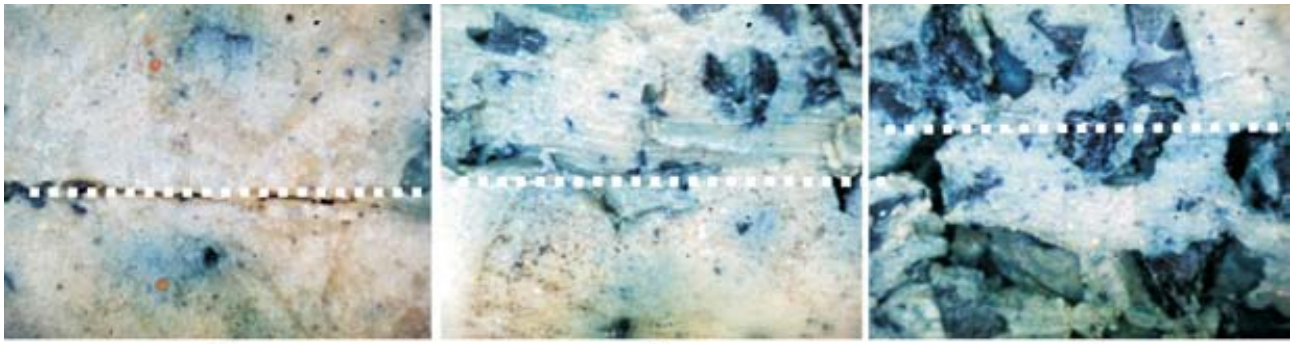

Figure 8 - Shear zones in specimens of BTN-TG mixtures (50x enlargement) at the end of tests with different values of tire grains content, (a) 25%, (b) 50% and (c) 75% of TG.

sion intercept varied between 7 kPa and 10 kPa (between 17% and 40% less than the value for the bentonite alone), depending on the material considered and its percentage in the mixture.

3.1.2. Consolidation, hydraulic conductivity and permittivity tests

The results obtained in consolidation tests on the bentonite mixtures are shown in Figs. 11(a) to (c) in terms of specimen vertical strain (equal to $\Delta e/(1 + e_o)$, where Δe is the void ratio variation and e_o is the initial void ratio) *vs.* vertical effective stress. For clarity sake the unloading stages of the tests are not presented in those figures. Greater expansions (negative values of $\Delta e/(1 + e_o)$) due to specimen inundation under the low initial vertical stress of 5 kPa were observed for the BTN-CLY mixtures (Fig. 11b). In spite of different initial values of vertical strain due to different expansion levels, the patterns of variation of e *vs.* σ of the mixtures are similar. The results obtained for the BTN-CLY specimens were little affected by the percentage of clay in the mixture, in contrast to what was observed for the other mixtures.

Table 6 presents results of hydraulic conductivity tests on bentonite mixture specimens for normal stresses

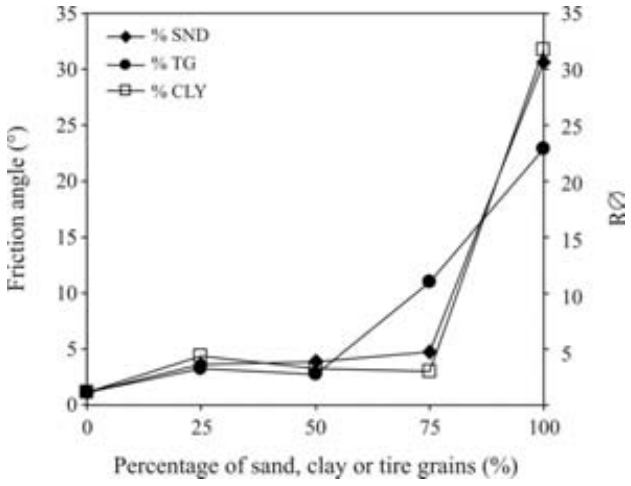

Figure 9 - Friction angles of bentonite mixtures after hydration.

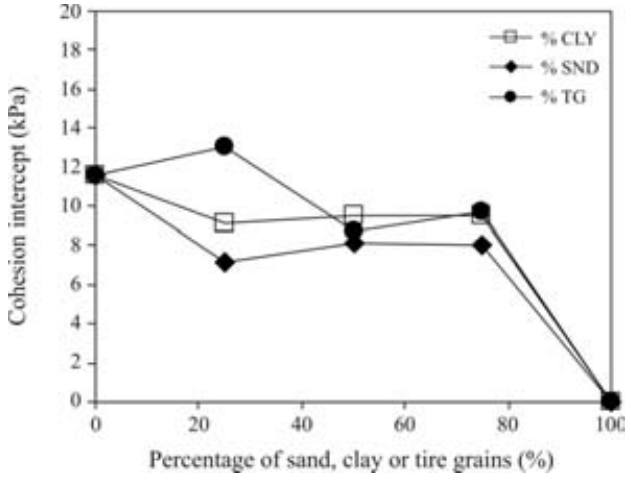

Figure 10 - Cohesion intercept obtained in direct shear tests on hydrated specimens.

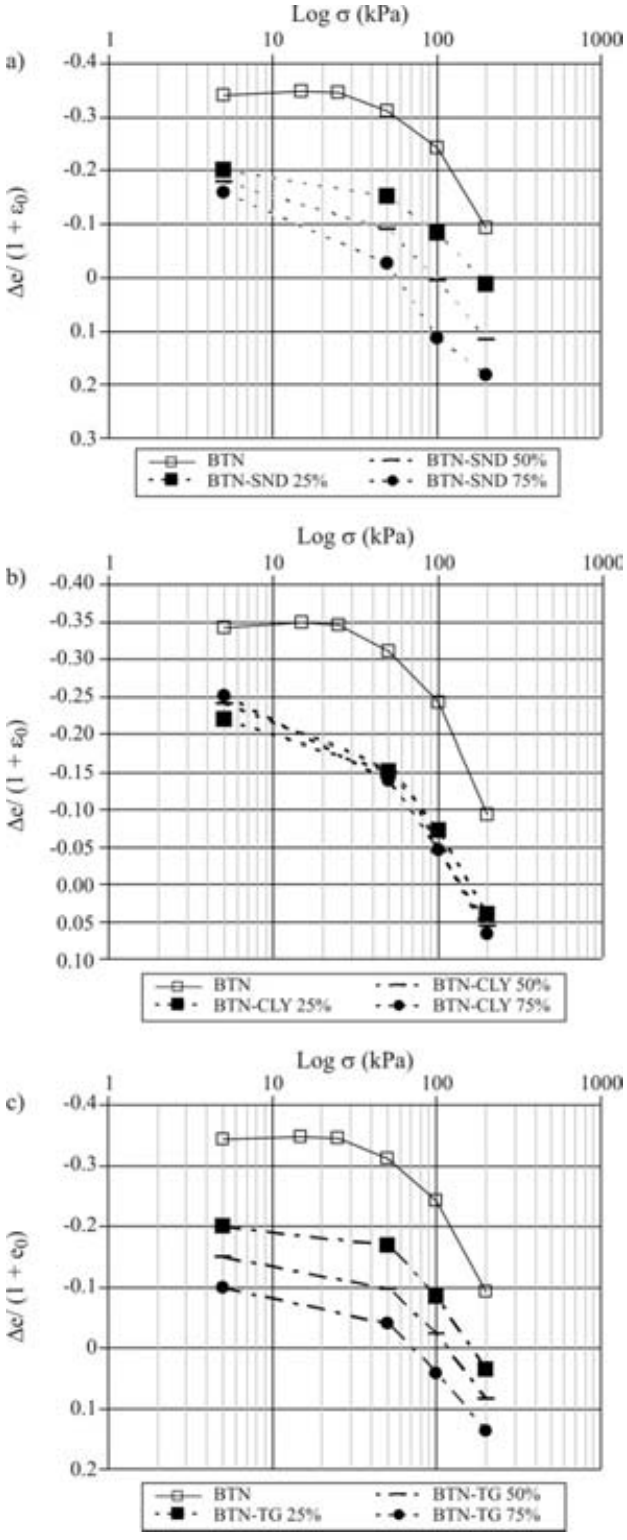

Figure 11 - Results of consolidation tests.

Table 6 - Hydraulic conductivity (k_N, cm/s) *vs.* normal stress (σ_N, kPa).

σ_N (kPa)	BTN (k_N x 10^{-9})	BTN-SND (k_N x 10^{-8})			BTN-CLY (k_N x 10^{-8})			BTN-TG (k_N x 10^{-8})		
		25%	50%	75%	25%	50%	75%	25%	50%	75%
50	3.3	2.3	2.3	2.4	5.2	4.6	5.2	3.4	4.0	4.9
100	3.0	1.4	2.3	1.1	2.0	1.0	2.1	2.0	1.6	4.2
200	2.0	1.4	2.3	1.1	2.0	1.0	2.1	1.6	1.6	2.1

varying from 50 kPa to 200 kPa. It can be noted that the hydraulic conductivity (k_N) of the bentonite alone was less sensitive to the normal stress than those of the mixtures. The values of k_N for the mixtures were 3.3 to 15.8 times greater than that of the bentonite alone, depending on the mixture and normal stress considered.

The hydraulic conductivity alone is not sufficient to assure a good performance of a material as a barrier, as its thickness plays also a fundamental role in the process. In this context, the permittivity (ratio between a medium hydraulic conductivity and its thickness, ψ) of the material provides a better measurement of the difficulty that a fluid will face to cross it. Figures 12 and 13 show the variations of permittivity and of permittivity ratio (R_ψ, ratio between mixture permittivity and bentonite permittivity) with normal stress, respectively, obtained from consolidation tests. A rather large scatter of test results can be observed and this is a consequence of the natural scatter of results of hydraulic conductivity in permeability tests, associated with the variability of the initial thickness of the mixtures under very loose states, depending on the type and content of the alternative material used. Figure 12 shows that the permittivity of the bentonite alone is less sensitive to the normal stress (ψ varying between 1.1 x 10^{-10} s^{-1} and 2.6 x 10^{-10} s^{-1}). For the bentonite mixtures, ψ varied between 7.4 x 10^{-9} s^{-1}, for the BTN-SND 75% mixture under 5 kPa normal stress (Fig. 12a) and to 6 x 10^{-10} s^{-1}, for BTN-CLY 50% mixture under 200 kPa normal stress (Fig. 12b). The ratio (R_ψ) between permittivity values of the mixture and of the bentonite alone varied between 5 and 29 (Figs. 13a to c), depending on the mixture and stress level considered. For a normal stress of 200 kPa the mixture permittivity was 5 to 12 times greater than that of the bentonite alone, depending on the alternative material considered, with lower values of ψ for mixtures of bentonite with clay. Despite the greater permittivity values of the mixtures, the results obtained show that the use of bentonite mixtures may be interesting in less critical barrier problems, particularly under stress levels greater than 100 kPa.

As permittivity is a function of the layer thickness, for larger thicknesses than the ones tested in the present study significantly lower values of permittivity could be obtained for the mixtures. Thus, thicker layers of bentonite-alternative material mixtures could function as a barrier as well as traditional (even thicker) compacted clay layers. In this sense, thicker bentonite-tire grains mixtures would consume a greater number of tires, which would be beneficial to the environment regarding a better use for this type of

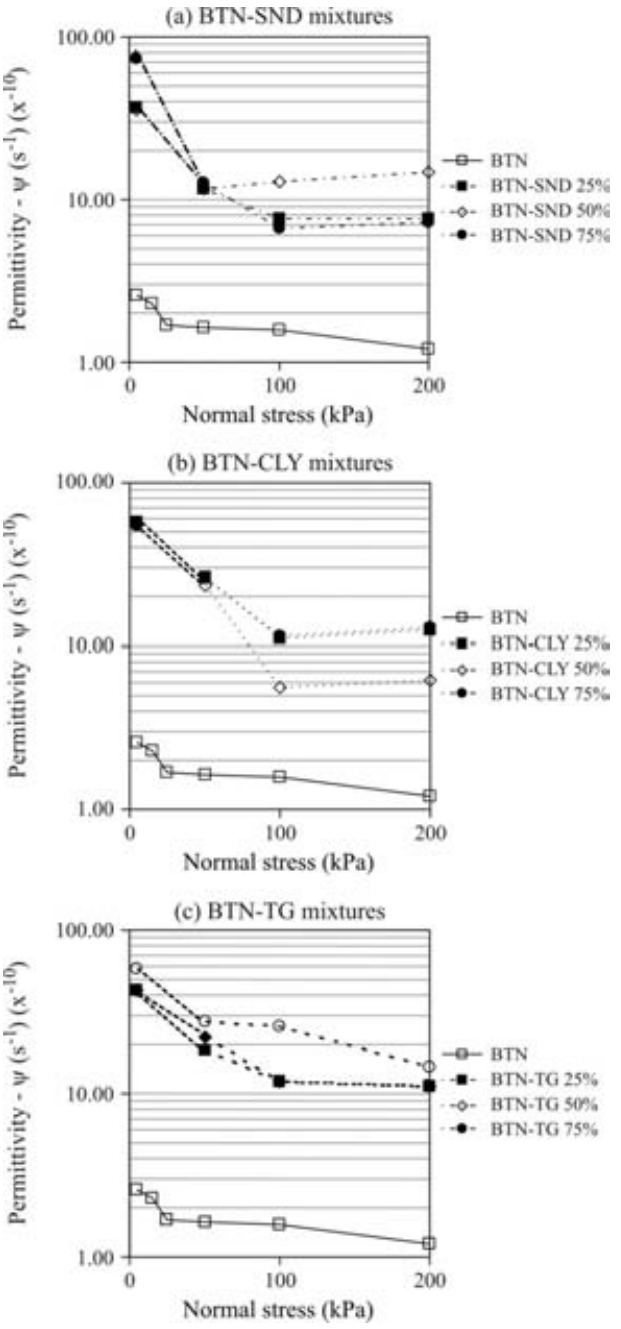

Figure 12 - Permittivity of mixtures *vs.* normal stress.

waste. However, obviously the cost of this alternative solution would have to be compared to those of other traditional solutions (compacted clay liner, GCL) to check its economical feasibility as a barrier.

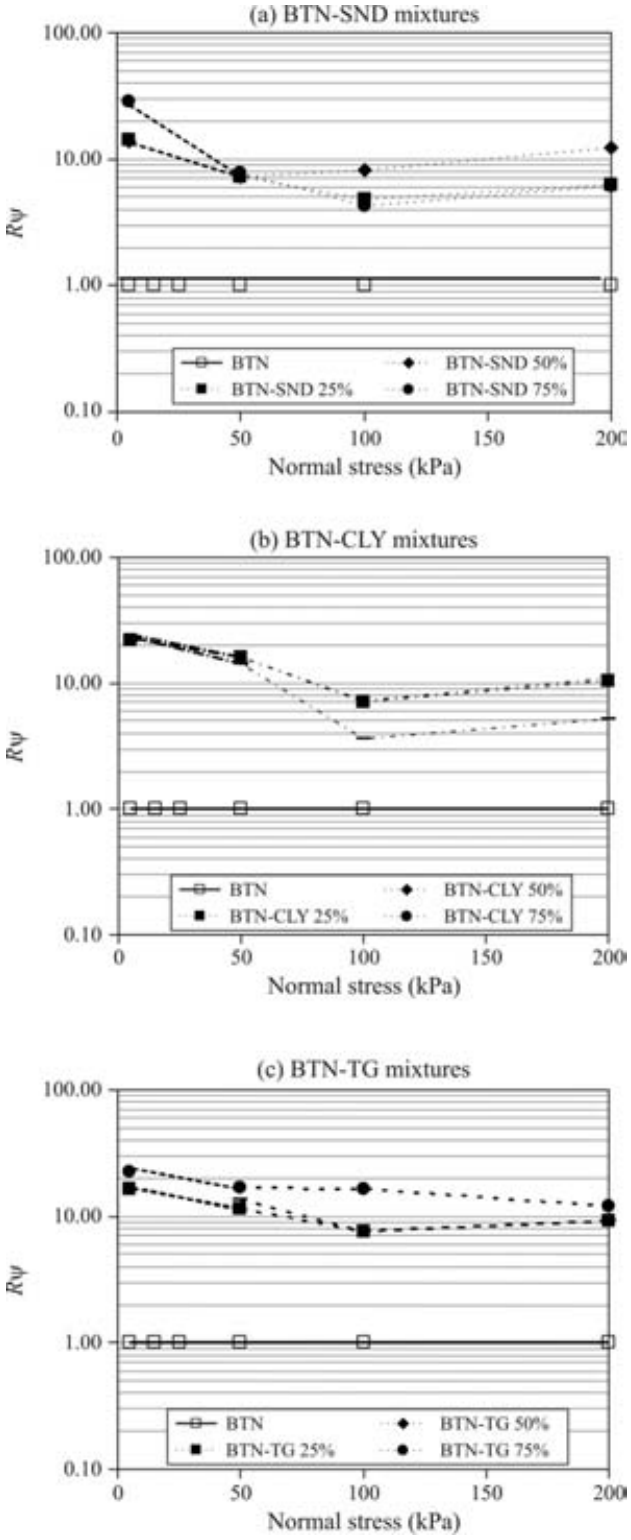

Figure 13 - Permittivity ratio *vs.* normal stress.

3.1.3. Expansibility tests

Figures 14(a) to (c) present the final relative expansion of the mixtures after 4 days under submersion in distilled water *vs.* confining normal stress (≤ 5 kPa). In these figures relative expansion is defined as the ratio between the specimen thickness increase and its initial thickness (prior to inundation). As expected, the expansibility of the mixture decreases with the increase of the amount of alter-

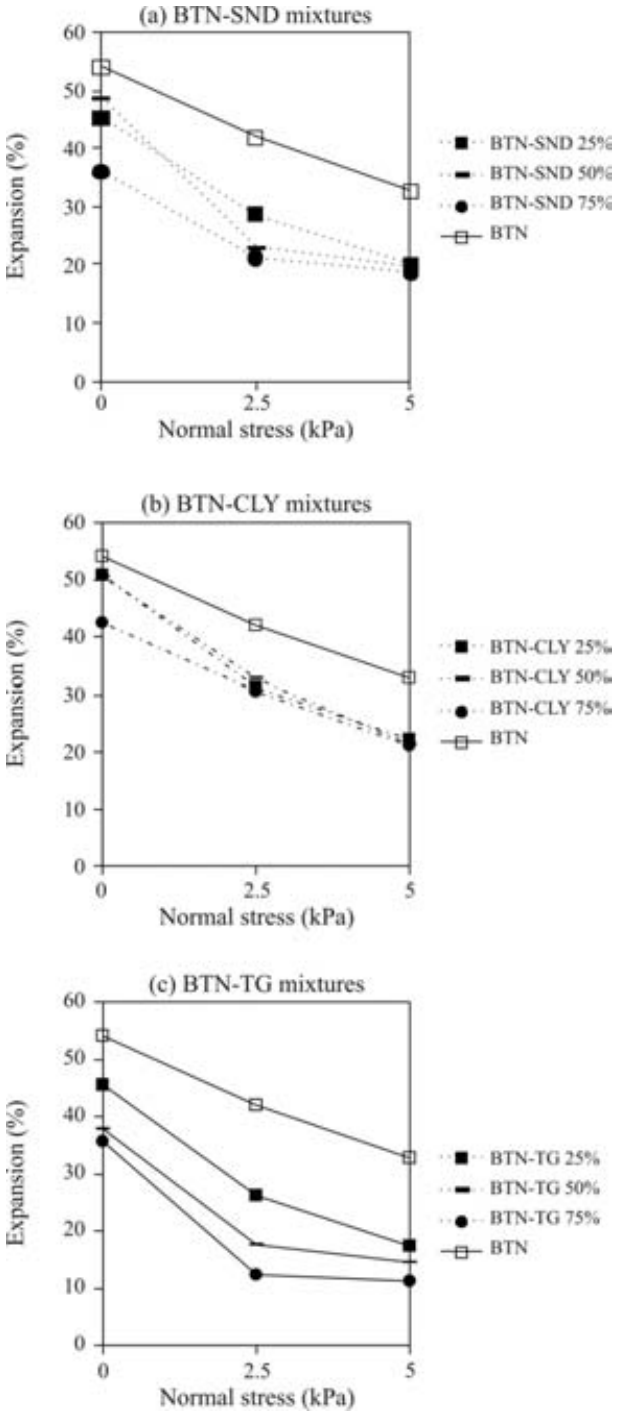

Figure 14 - Mixture expansion *vs.* normal stress.

native material in the mixture and with the increase of confining stress. The BTN-TG mixtures were the ones that presented the smallest expansions, which may be associated with the smaller water retention capacity and large initial void ratios of these mixtures.

Figure 15 shows the value of the ratio (R_e) between the final expansion of the mixture and the final expansion of the bentonite alone for each mixture tested. As expected, R_e decreased with the confining stress and, for a given alternative material, with the percentage of that material in the mixture. A more significant reduction on the value of R_e with the percentage of alternative material in the mixture was observed for the BTN-TG mixtures. This is in part a consequence of the smaller dry specific unit weight of this mixture.

3.2. Performance of GCLs with alternative core materials

3.2.1. Tests on alternative GCLs

Based on the results of the tests carried out on the bentonite mixtures presented in the previous section, a 50% percentage in mass of alternative material was chosen for the production of the alternative GCLs. This percentage is a compromise between the use of a great percentage of the alternative material in the mixture and less losses of relevant geotechnical and hydraulic parameters for barrier systems. Three alternative GCLs (GCL-SND 50%, GCL-CLY 50% and GCL-TG 50%) and the conventional GCL A and B were subjected to free expansion tests and to ramp tests (0.6 m x 1.0 m size specimens).

3.2.1.1. Free expansion tests

Figure 16 presents the results obtained in the free expansion tests performed. This figure shows that the GCLs with cores resulting from the mixtures of bentonite and alternative materials (50% in mass) presented less expansion than that of the conventional commercial products GCL A and GCL B. This was a consequence of the non expansive

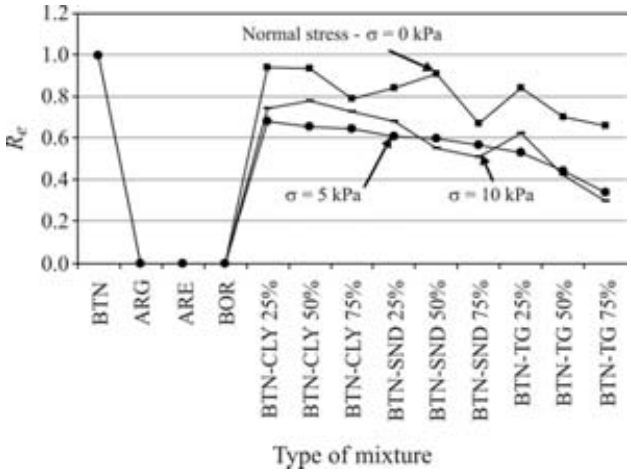

Figure 15 - Value of the ratio R_e for different types of mixtures.

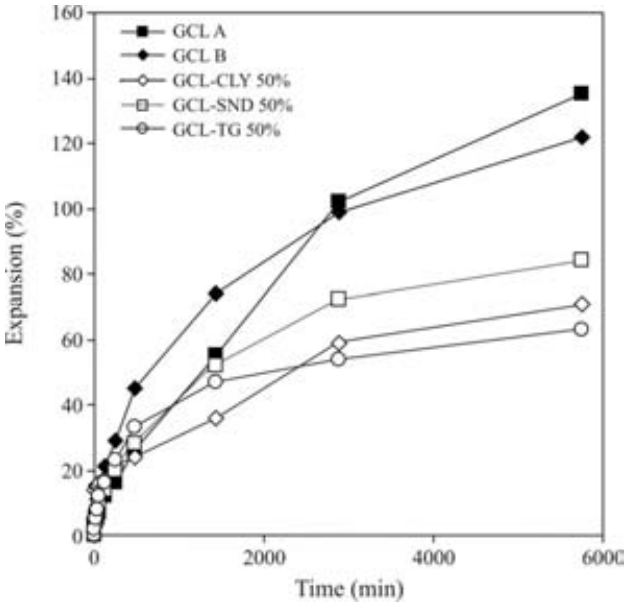

Figure 16 - GCL free expansion *vs.* time.

nature of the alternative materials employed. GCL BTN-TG 50% was the one showing less expansion, of the order of half the expansion observed for the conventional products.

3.2.1.2. Ramp tests

Figure 17 shows the relationship between shear stress and normal stress on the GCL under dry conditions and after hydration for 24 h ("H") obtained at the end of the ramp tests. It is important to point out that only for GCL B tested after hydration this relationship represents a failure envelope, because of internal shear failure having been reached in this case. For the other products tested internal failure was not obtained in the ramp tests because of the contribution from the stitches' strength. In these cases, the maximum inclination imposed to the ramp was of the order of 50°. As a result, for a given normal stress, similar mobilized shear stresses were obtained for GCL A (dry or hydrated), GCL B (dry) and the alternative GCLs. This shows that for the conditions of the test the presence of the alternative materials did not influence the GCL internal strength, in part because in these cases the internal shear strength was controlled by the strength of the stitches. For the same reason, hydration had little effect on the behaviour of the alternative GCLs in comparison with the reference commercial GCLs used in this experimental programme.

The stitch filaments can have a marked effect on the internal shear strength and on the shear stiffness of the GCL. For the ramp tests carried out, internal failure occurred only for hydrated GCL B. In this case, it was observed that the expansion of the bentonite of GCL B caused failure of some stitches, which yielded to lower internal shear strength. This reduction on the internal shear strength of the GCL may compromise the stability of the lining sys-

tem in a slope, if this aspect is not properly considered in the design. Figures 18(a) and (b) show enlarged views of stitches in GCLs A and B, respectively. Figure 18(b) shows a stitch filament that failed during hydration of GCL B. This failure mechanism can be minimized or avoided if hydration takes place under high stress levels, because under such conditions the expansion of the bentonite will be inhibited to some extent. Therefore, the critical conditions will take place under low stress levels and in this case the ramp test on hydrated GCLs can provide important information on the internal strength of the GCL under normal stresses closer to those expected in the field.

Figure 19 presents maximum values of mobilized tensile load on the lower (carrier) geotextile of the GCL *vs.* normal stress at the end of the ramp tests. In all cases, except for hydrated GCL B, the mobilized tensile force increased with normal stress with little difference among results of tests on different GCLs. The results obtained for the GCL with BTN-TG 50% mixture were close to those of GCLA. The rather constant value of mobilized tensile load with normal stress for the hydrated GCL B was due to internal failure having occurred prior to significant mobilization of force in the carrier geotextile of this product.

The variation of shear displacement (difference between displacements of the cover and carrier geotextiles of the GCL) with normal stress at the end of the ramp tests is depicted in Fig. 20 for each GCL tested. It can be noted that hydration slightly increased the relative displacement between cover and carrier geotextiles of GCL A. Under dry conditions the variation of these displacements with normal stress was similar for GCLs A and B for normal stresses greater than 2.5 kPa. However, hydration caused catastrophic internal failure of GCL B, with relative displacements in excess of 100 mm. With the exception of GCL B

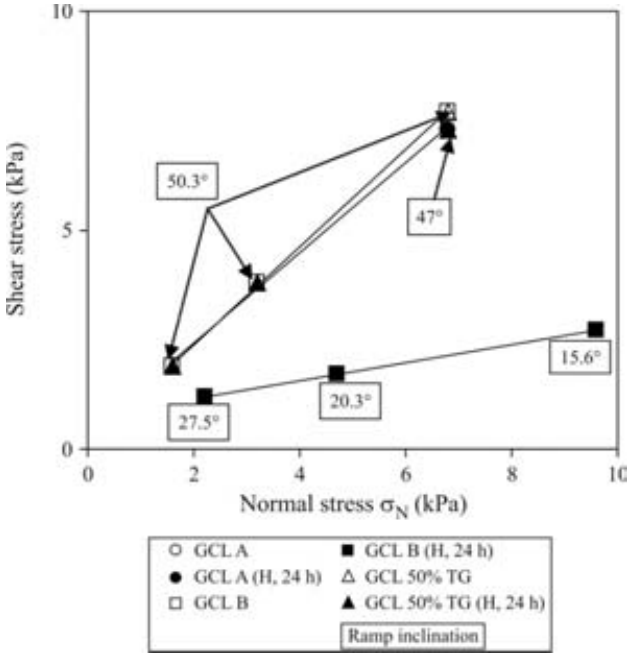

Figure 17 - Mobilised shear stress *vs.* normal stress on the GCL for dry and hydrated specimens.

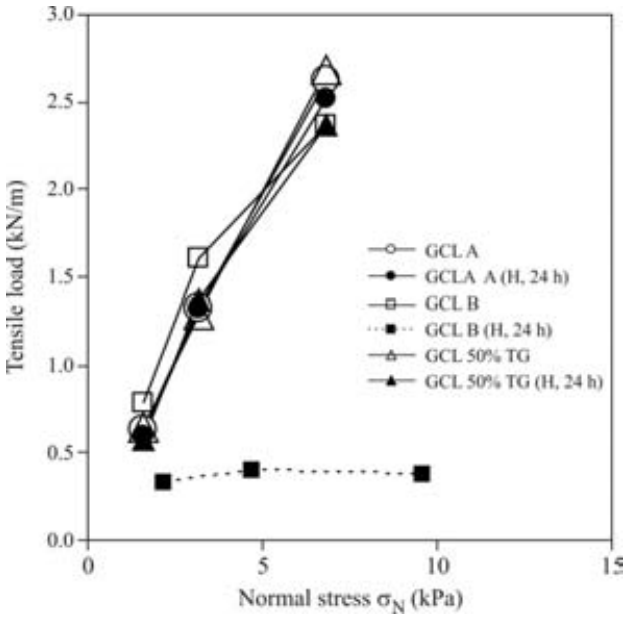

Figure 19 - Maximum mobilised tensile force *vs.* normal stress.

Figure 18 - Stitches of GSLs A and B after hydration: (a) GCL A stitch after hydration; (b) Failed stitch in GCL B after hydration.

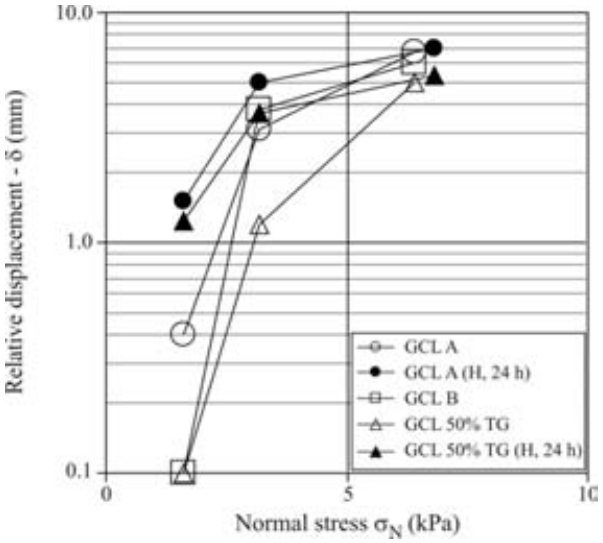

Figure 20 - Relative displacement *vs.* normal stress in ramp tests.

(H, 24 h), the maximum relative displacement for the range of normal stresses used was approximately 7 mm. Similar results of maximum relative displacements were obtained for the alternative GCLs independent on the material (tire grains, sand or clay) mixed to the bentonite, with maximum values below 5.5 mm for dry and hydrated conditions. Great distortions of the GCL will increase the deformation of the lining system as a whole, which may favour the formation of cracks in compacted soil layers overlying the GCL and increase the tensile load in the geomembrane (if present) on the GCL at the anchorage region.

4. Conclusions

This paper presented results of a laboratory study on the use of alternative materials mixed to bentonite in GCLs. The main conclusions obtained are summarised below.

The presence of the alternative materials (sand, clay or tire grains) increased the shear strength of the mixture. For the mixture with tire grains the shear strength increase was observed at the late stages of direct shear tests, mainly due to the compressible nature of the tire grains, which increased the deformability of the mixture. The friction angles of the mixtures were also greater than that of the bentonite alone under dry and hydrated conditions, although for the latter condition the values were still low. Under hydrated conditions, the cohesion intercept obtained for the mixtures were smaller than that of the bentonite alone, being between 17% and 40% smaller than the value obtained for the bentonite, depending on the mixture considered.

The compressibility of the mixtures was greater than that of the bentonite. This was due to the loose state of the specimens tested and compressibility of individual grains, like in the case of the tests with tire grains.

The addition of alternative materials to the bentonite reduced the expansibility and increased the permittivity of the mixture. Permittivity values of the mixtures were 5 to 29 times greater than that of the bentonite alone, depending on the mixture and stress level considered. In general, the greatest increases on permittivity were observed for the bentonite-tire grains mixtures. Even so, the permittivity of bentonite-tire grains mixtures for percentages (in mass) of tire grains up to 50%, and normal stresses above 100 kPa, were of the order of 10^{-9} s^{-1} (0.18×10^{-9} s^{-1} for the bentonite alone). The expansions of the hydrated alternative GCLs manufactured in the laboratory were also smaller than those of the two commercial conventional GCLs tested.

The internal shear strength, as measured in ramp tests, was controlled by the strength of the stitches of the GCLs. Only commercial GCL B failed in this type of test. The results obtained for the alternative GCL made with core consisting of a mixture of bentonite and tire grains (50% in mass) were similar to those presented by commercial GCL A, under dry and hydrated conditions, in terms of mobilised shear stresses and mobilised tensile loads in the carrier geotextile.

The results obtained showed that the mixture of the alternative materials used in this research programme with bentonite can increase the internal shear strength of an alternative low cost GCL made with those mixtures, but degraded some other important parameters for barrier applications, such as GCL expansibility and permittivity. Increases in the cost of manufacturing the alternative GCLs should also be taken into account before assuming that the use of less bentonite alone will result in a cheaper GCL, particularly for the case o mixtures involving bentonite and sand. Some practical aspects also need investigation, such as the possibility of segregation of the alternative material used in the GCL during transportation, handling and installation in the field. This segregation can be minimised or avoided depending on the manufacturing process used to produce the GCL, but this can also yield to additional costs to produce the alternative GCL product.

Despite presenting greater permittivity and lower expansibility than conventional GCLs, alternative products with mixtures of bentonite and tire grains may be considered for less critical barrier systems and as bedding/protective layers underneath geomembranes, particularly under confining stresses above 100 kPa, which are easily reached in waste disposal areas. In addition, this type of use of tire grains provides a more environmentally friendly use of wasted tires. However, despite some encouraging results obtained in this work, further research is required for a better understanding on the behaviour of alternative GCL products.

References

ASTM D 6243 (2009) Standard test method for determining the internal and interface shear resistance of geo-

synthetic clay liner by the direct shear method. ASTM International, West Conshohocken, PA, USA.

ASTM D 4595 (2009) Standard Test Method for Tensile Properties of Geotextiles by the Wide-Width Strip Method. ASTM International, West Conshohocken, PA, USA.

ASTM D4491 (2009) Standard Test Methods for Water Permeability of Geotextiles by Permittivity. ASTM International, West Conshohocken, PA, USA.

Bouazza, A. (2002) Review article: geosynthetic clay liners. Geotextiles and Geomembranes, v.20, 13, pp. 3-17.

Bouazza, A. & Vangpaisal, T. (2007) Gas permeability of GCLs: effect of poor distribution of needle-punched fibres. Geosynthetics International, v. 14:4, p. 127-142.

Chiu, P. & Fox, P.J. (2004) Internal and interface shear strengths of unreinforced and needle-punched geosynthetic. Geosynthetics International, v. 11:3, p. 176-199.

Didier, G & Al Nassar, M. (2002) Hydraulic performance of geosynthetic clay liners some French laboratory test methods. Clay Geosynthetics Barriers. Zanzinger, Koerner, Gartung (eds), pp. 249-273.

Fox, P.J.; Rowland., M.G. & Scheithe, J.R. (1998) Internal shear strength of three geosynthetic clay liners, Journal of Geotechnical and Geoenvironmental Engineering, ASCE, v. 124:10, p. 933-944.

Fox, P.J. & Stark, T.D. (2004) State-of-the-art report: GCL shear strength and its measurement. Geosynthetics International, v. 11:3, p. 117-151.

Ikizler, S.B.; Aytekin, M. & Vekli, M. (2009) Reductions in swelling pressure of expansive soil stabilized using EPS geofoam and sand. Geosynthetics International, v. 16:3, p. 216-221.

Koerner, R.M. (2005) Design with geosynthetics. 5th ed. Prentice Hall New Jersey, USA, 816 pp.

Müller, W.; Jakob, I.; Seeger, S. & Tatzky-Gerth, R. (2008) Long-term shear strength of geosynthetic clay liners. Geotextiles and Geomembranes, v. References and further reading may be available for this article. To view references and further reading you must this article. 26:2, p. 130-144.

NF EN ISO 12956 (2010) Géotextiles et produits apparentés – Détermination de l'ouverture de filtration caractéristique.

Palmeira, E.M. (2009) Soil-geosynthetic interaction: modelling and analysis. Geotextiles and Geomembranes, v. 27:5, p. 368-390.

Palmeira, E.M.; Lima Junior, N.R. & Mello, L.G. (2002) Interaction between soil and geosynthetic layers in large scale ramp tests. Geosynthetics International, v. 2:9, p. 149-187.

Palmeira, E.M. & Viana, H.N.L (2003) Effectiveness of geogrids as inclusions in cover soils of slopes of waste disposal areas. Geotextiles and Geomembranes, v. 21:5, p. 317-337.

Reuter E. & Markwardt N. (2002) Design of landfill cover lining systems with geosynthetic clay liners (GCLs). 7th International Conference on Geosynthetics, Nice, France, v. 1, pp. 573-576.

Rowe, R.K. & Orsini, C. (2003) Effect of GCL and subgrade type on internal erosion in GCLs under high gradients, Geotextiles and Geomembranes, v. 21:1, p. 1-24; References and further reading may be available for this article. To view references and further reading you must this article.

Shan, H-Y & Daniel, D. E. (1991) Results of laboratory tests on a geotextile/bentonite liner material. Geosynthetics 91', IFAI, Atlanta, GA, v. 2, pp. 517-535.

Shan, H,Y. & Chen, R.H. (2003) Effect of gravel subgrade on hydraulic performance of geosynthetic clay liner. Geotextiles and Geomembranes, v. 21:6, p. 339-354.

Sivakumar Babu, G.L., Sporer, H., Zanzinger, H. & Gartung, E. (2001) Self-healing properties of geosynthetic clay liners. Geosynthetics International, v. 8:5, p. 461-470.

Thiel, R.; Daniel, D. E.; Erickson, R. B.; Kavazanjian, E. Jr & Giroud, J.P. (2001) The GSE GundSeal GCL Design Manual, GSE Lining Technology, Inc., Houston, TX, USA.

Touze-Foltz, N.; Duquennoi, D. & Gaget, E. (2006) Hydraulic and mechanical behavior of GCLs in contact with leachate as part of a composite liner. Geotextiles and Geomembranes, v. 24:3, p. 188-197.

Viana, H.N.L. (2007) A study on the stability and hydraulic conductivity of conventional and alternative barrier systems for waste disposal areas, PhD. Thesis, Graduate Programme of Geotechnics, University of Brasilia, 201 pp. (in Portuguese).

Viana, H,N.L. & Palmeira, E.M. (2010) Influence of geogrid geometrical and mechanical properties on the performance of reinforced veneers. Soils and Rocks, v. 33:1, p. 33-44.

Viana, P.M.F. & Palmeira, E.M. (2009) Evaluation of GCL internal shear strength in inclined plane tests. GeoAfrica 2009, Cape Town, South Africa, 8 pp.

Viana, P.M.F. & Palmeira, E.M. (2008) Evaluation of the interface and internal strength of alternative barrier systems incorporating geosynthetics. Internal Report, Graduate Programme of Geotechnics, University of Brasilia, Brazil, 57 pp. (in Portuguese).

Volume 34, N. 1, January-April 2011

Table of Contents